AD_____

Award Number: W81XWH-09-1-0583

TITLE: Deregulation of miRNAs contributes to development and progression of prostate cancer

PRINCIPAL INVESTIGATOR: Ralph W. deVere White, M.D.

CONTRACTING ORGANIZATION: University of California
Davis, CA 95616

REPORT DATE: September 2012

TYPE OF REPORT: Final

PREPARED FOR: U.S. Army Medical Research and Materiel Command
Fort Detrick, Maryland 21702-5012

REPORT DOCUMENTATION PAGE

Form Approved
OMB No. 0704-0188

1. REPORT DATE	**2. REPORT TYPE**	**3. DATES COVERED**
September 2012	Final	15 August 2009 – 14 August 2012

4. TITLE AND SUBTITLE

Deregulation of miRNAs contributes to development and progression of prostate cancer

5a. CONTRACT NUMBER

5b. GRANT NUMBER
W81XWH-09-1-0583

5c. PROGRAM ELEMENT NUMBER

6. AUTHOR(S)

Ralph W. deVere White, M.D.

E-Mail: rwdeverewhite@ucdavis.edu

5d. PROJECT NUMBER

5e. TASK NUMBER

5f. WORK UNIT NUMBER

7. PERFORMING ORGANIZATION NAME(S) AND ADDRESS(ES)

University of California
Davis, CA 95616

8. PERFORMING ORGANIZATION REPORT NUMBER

9. SPONSORING / MONITORING AGENCY NAME(S) AND ADDRESS(ES)
U.S. Army Medical Research and Materiel Command
Fort Detrick, Maryland 21702-5012

10. SPONSOR/MONITOR'S ACRONYM(S)

11. SPONSOR/MONITOR'S REPORT NUMBER(S)

12. DISTRIBUTION / AVAILABILITY STATEMENT
Approved for Public Release; Distribution Unlimited

13. SUPPLEMENTARY NOTES

14. ABSTRACT

In the 3rd year of this grant, we further explored the role miR-125b plays in CaP pathogenesis and found that miR-125b targets the tumor suppressive gene p14ARF. We also performed animal studies to validate our previous finding that miR-125b contributes to tumorigenesis of CaP. Furthermore, we observed that targeting miR-125b using anti-miR-125b inhibits growth of CaP tumors and sensitizes CaP cells to the anti-CaP drug Taxol. In addition, we examined 133 clinical prostate samples, and found that an increased miR-125b level is common in clinical CaP samples, which may be associated with CaP progression. These findings, together with those in the first and second year, support our hypothesis that miR-125b acts as an oncogene, contributing to the development and progression of CaP. Therefore, targeting miR-125b may represent a new strategy for improved CaP treatment.

15. SUBJECT TERMS
miRNA, tumorigenesis, oncogene, prostate cancer, Bak1, Puma p53

16. SECURITY CLASSIFICATION OF:			**17. LIMITATION OF ABSTRACT**	**18. NUMBER OF PAGES**	**19a. NAME OF RESPONSIBLE PERSON**
a. REPORT	**b. ABSTRACT**	**c. THIS PAGE**			USAMRMC
U	U	U	UU	44	**19b. TELEPHONE NUMBER** *(include area code)*

Table of Contents

a. Introduction

The subject of the research is "Deregulation of miRNAs contributes to development and progression of prostate cancer". The overall hypothesis of this grant is that *miR-125b* acts as an oncogene, contributing to the development and progression of prostate cancer. In this study, we proposed to test the ability of aberrantly-expressed *miR-125b* to promote tumorigenesis and to induce AI growth in three specific aims. Aim 1 is to elucidate the mechanism by which *miR-125b* contributes to pathogenesis of prostate cancer. Aim 2 is to evaluate the effects of *miR-125b* on prostatic tumorigenesis and AI growth. Aim 3 is **t**o determine the application of *miR-125b* as a biomarker for prostate cancer. This is the annual report for our studies performed during the 3rd year.

b. Body

In the 3rd year, the studies performed include: 1) further exploration of the role *miR-125b* plays in CaP pathogenesis, 2) validating the contribution of *miR-125b* to tumorigenesis of CaP by alteration of cellular abundance of *miR-125b*, and 3) analyzing clinical samples for the expression level of *miR-125b*. The following studies have been performed and expected results been obtained.

1. ***miR-125b* down-regulates p14^{ARF} in CaP cells.** Previous studies demonstrated that tumor suppress gene p14^{ARF} is significantly downregulated in CaP tissues (1). How p14^{ARF} is downregulated remained poorly understood. Since the 3'UTR of p14^{ARF} gene contains a potential *miR-125b* binding site, we investigated the effect of *miR-125b* on the regulation of p14^{ARF} in CaP cells. Both LNCaP and 22R*v*1 cells were transfected with synthetic *miR-125b* or with anti-*miR-125b*, and the level of p14^{ARF} was detected by Western blot analysis. We observed an 80% decrease of p14^{ARF} level in LNCaP and 60% in 22R*v*1 (**Fig. 1A**). Conversely, anti-*miR-125b* (antisense inhibitor of *miR-125b*) increased the p14^{ARF} level by 40% in LNCaP and 30% in 22R*v*1 (**Fig. 1A**). Additionally, we examined lenti-*miR-125b* PC-346C xenograft tumor that highly expresses *miR-125b*, and found a 60% reduction of p14^{ARF} protein (**Fig. 1B**). To determine that the putative *miR-125b* binding site is responsible for the regulation of p14^{ARF} by *miR-125b*, the luciferase reporter vectors containing the 3' UTR of *p14^{ARF}* gene were co-transfected with *miR-125b* into LNCaP cells. Cotransfection resulted in approximately 50% reduction of the enzyme activity (**Fig. 1C**), indicating that the 3' UTR of *p14^{ARF}* is the target of *miR-125b.* Taken together, these results validate the regulation of p14^{ARF} by *miR-125b* in CaP cells.

2. ***miR-125b* regulates p14^{ARF}/mdm2/p53 signaling pathway**. Since p14^{ARF} accelerates mdm2 degradation, resulting in p53 up-regulation (2), we performed three experiments to determine whether *miR-125b* regulates the p14^{ARF}/mdm2/p53 signaling pathway. ***1***) LNCaP and 22R*v*1 cells were treated with synthetic *miR-125b* and the levels of mdm2 and p53 were examined by Western blot analysis. Compared with the negative control (miR-NC), *miR-125b* induced an increased mdm2 and a reduced p53 in LNCaP and 22Rv1 cells (**Fig. 2A**). As expected, *miR-125b*-mediated downregulation of p53 induced significantly reduced expression of two direct p53 effectors: p21^{Cip1} and Puma. ***2***) To confirm the inhibition effects of *miR-125b* on p14^{ARF}/mdm2/p53 signaling, we used p14^{ARF} siRNA (sip14) to silence p14^{ARF} expression in LNCaP and 22R*v*1 cells and analyzed the levels of p14^{ARF}, p53 and mdm2. It was found that sip14 treatment significantly decreased the expression of p14^{ARF} and subsequently upregulated mdm2 level and downregulated the expression of p53 (**Fig. 2B**). ***3***) Since p14^{ARF} directly binds to the C-terminal of mdm2, we examined the effect of *miR-125b* on the interaction between p14^{ARF} and mdm2 by co-IP in R22R*v*1 cells. We observed that mdm2 can be detected from anti-p14^{ARF}-precipitated proteins, not from control IgG-coupled proteins (**Fig. 2C**), indicating that endogenous p14^{ARF} is capable of forming a complex with mdm2. Treatment with *miR-125b* downregulated p14^{ARF}protein, resulting in a reduction of immunoprecipitated mdm2. These data suggest that *miR-125b* regulates p14^{ARF}/mdm2/p53 signaling pathway

3. ***miR-125b*-p14^{ARF}signaling mediates p53-independent growth inhibition**. Studies have demonstrated that a portion of clinical CaPs have inactive p53 (3). We studied whether *miR-125b/*p14^{ARF} regulates apoptosis in these p53-inactivated CaP cells. To address this issue, a p53-null PC3 CaP cell model was utilized. We first

tested the regulation of $p14^{ARF}$/mdm2 signaling by *miR-125b* in PC3 cells. Similar to p53-positive cells, *miR-125b* treatment decreased expression of $p14^{ARF}$ by 36% and increased mdm2 by 43% (**Fig. 3A**). Since PC3 cells express the apoptotic factor Puma that is a direct target of *miR-125b*, *PUMA* was first knocked down using siRNA to Puma (siPuma). Cells were then transfected with *miR-125b* and a WST-1 assay was used to assess the effect of *miR-125b* on cell proliferation. Data from WST-1 assay revealed that *miR-125b* treatment induces 2-fold increase in survival of PC3 cells (**Fig. 3B**). We then tested whether an anti-*miR-125b* treatment induced apoptotic cell death in Puma-silenced PC3 cells. Tunel assay demonstrated that approximately 50% of the cells treated with anti-*miR-125b* underwent apoptosis (**Fig. 3C**). Therefore, our data suggest that *miR-125b/*$p14^{ARF}$ plays a role in regulation of apoptosis in p53-inactivated CaP cells.

4. ***miR-125b* facilitates growth of CWR22 tumors while anti-*miR-125b* inhibited growth of CWR22 xenografts tumors**. In a previous study (4), we found that *miR-125b* stimulated growth of PC-346C tumors. We validated this finding in a CWR22 xenograft model. To do this, CWR22 cell suspensions were injected *s.c* into nude mice implanted with time-release testosterone pellets. Mice then were treated with polyethylenimines (PEI)-complexed *miR-125b* (PEI-miR-125b) and miRNA negative control (PEI-miR-NC). PEI (polyplus-transfection Inc.) can form complexes with miRNA, increase internalization and facilitate miRNA release from endosomes into cytoplasm (5). The goal of the study was to determine if PEI is able to deliver chemically synthetic *miR-125b* (Ambion), as well as anti-miR-*125b*, into CaP cells *in vivo*. Consistent with previous PC-346C tumor, treatment with PEI-*miR-125b* promoted growth of CWR22 xenograft tumors (**Fig. 4A**). We then tested whether inactivation of *miR-125b* with synthetic anti-*miR-125b* inhibits the growth of CWR22 tumor. To this end, anti-*miR-125b* (Ambion) was mixed with PEI and *i.v.* injected into nude mice bearing ~50 mm^3 CWR22 xenograft tumor. We observed tumor-inhibitory effects in mice treated with PEI-complexed anti-*miR-125b* (**Fig. 4B**). In this experiment, another group of mice bearing CWR22 tumors were treated with PEI-complexed anti-*miR-125b* plus Taxol. It was found that PEI-anti-*miR-125b* significantly increased the therapeutic efficiency of Taxol (**Fig. 4B**). Our data suggests that PEI facilitates entry of synthetic *miR-125* and anti-*miR-125b* into tumor cells, and *miR-125b* facilitates growth of CWR22 tumors while anti-*miR-125b* inhibited growth of CWR22 xenografts tumors.

5. **Clinical CaP tissues highly express *miR-125b*.** In order to determine the clinical significance of *miR-125b*, we recently examined its expression levels in 133 prostate tissues (46 BPHs and 87 CaPs) using qPCR. We observed elevated *miR-125b* levels in CaP samples when compared with the BPH (**Fig. 5A**). The average *miR-125b* level was 3.0-fold greater in the CaP than the BPH. Since clinical information (serum PSA level and Gleason score) is available in 42 CaPs, we determined whether *miR-125* abundance correlates with the Gleason score of CaPs or serum PSA level. Although no correlation between *miR-125b* abundance and the PSA level was observed (data not shown), the *miR-125* levels do correlated with patients' Gleason scores (103 ± 18 relative fold in Gleason score 5-6 vs 160 ± 16 in Gleason score 7-10, $p=0.03$) (**Fig. 5B**). Therefore, these data suggest that *miR-125b* contributes to pathological progression of CaP.

c. Key Research Accomplishments

The key accomplishments include: ***1***) *miR-125b* directly targets $p14^{ARF}$ and *miR-125b*/$p14^{ARF}$ signaling may contribute to development and progression of CaP. Moreover, *miR-125b*/$p14^{ARF}$ signaling may play a role in promoting growth of p53-negative CaP tumor. A manuscript is being prepared to present our data. ***2***) Data from animal experiments validate our previous finding that *miR-125b* contributes to the pathogenesis of CaP. Therefore, targeting *miR-125b* may represent a new strategy for improved CaP treatment. ***3***) We examined a large number of clinical samples, and found that increased expression of *miR-125b* is common in CaPs, which may be associated with CaP progression.

d. Reportable Outcomes

In the third year, one paper has been published that elucidates the regulation of *miR-125b* by *miR-124* in CaP. In addition, a manuscript is being prepared that presents our current finding that *miR-125b* regulates $p14^{ARF}$/mdm2

signaling pathway. This regulation provides mechanistic explanation for reduced p53-dependent apoptosis in p53-inactivated CaP cells.

- Shi XB, Xue L, Ma AH, Tepper CG, Gandour-Edwards R, Kung HJ, deVere White RW. Tumor suppressive *miR-124* targets androgen receptor and inhibits proliferation of prostate cancer cells. Oncogene, 2012 (in press).

e. Conclusion

In the third year, we found that: ***i***) *miR-125b* directly targets another tumor suppressive gene $p14^{ARF}$; *ii*) inactivation of *miR-125b* using synthetic anti-*miR-125b* inhibits the growth of CaP xenograft tumor; and *iii*) *miR-125b* is highly expressed in clinical CaP samples. Together with results obtained in the first and second year, our data supports our hypothesis that *miR-125b* acts as an oncogene, contributing to the development and progression of prostate cancer. Therefore, targeting *miR-125b* may represent a new strategy for improved CaP treatment.

References

1. Konishi N, Nakamura M, Kishi M, Nishimine M, Ishida E, Shimada K. Heterogeneous methylation and deletion patterns of the INK4a/ARF locus within prostate carcinomas. Am J Pathol. 160:1207, 2002.
2. Zhang Z, Wang H, Li M, Rayburn ER, Agrawal S, Zhang R. Stabilization of E2F1 protein by MDM2 through the E2F1 ubiquitination pathway. Oncogene. 24:7238, 2005.
3. Nesslinger NJ, Shi XB, deVere White RW. Androgen-independent growth of LNCaP prostate cancer cells is mediated by gain-of-function mutant p53. 63:2228, Cancer Res. 2003.
4. Shi XB, Xue L, Ma AH, Tepper CG, Kung HJ, White RW. miR-125b promotes growth of prostate cancer xenograft tumor through targeting pro-apoptotic genes. The Prostate,71:538, 2011.
5. Boussif O, Lezoualc'h F, Zanta MA, Mergny MD, Scherman D, Demeneix B, et al. A versatile vector for gene and oligonucleotide transfer into cells in culture and in vivo: polyethylenimine. Proceedings of the National Academy of Sciences of the United States of America. 1995;92:7297-301.

Appendices

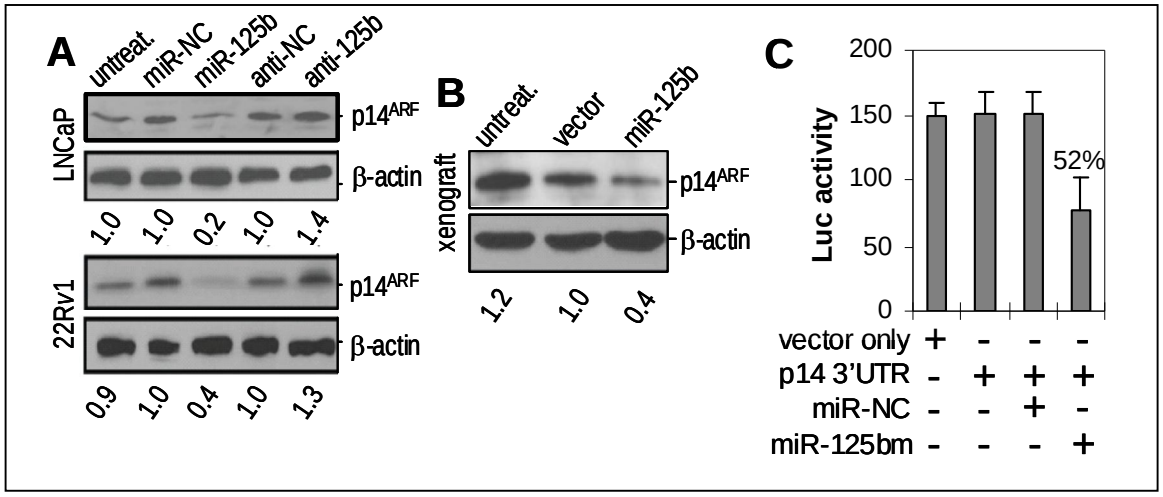

Figure1: *MiR-125b* targets p14^{ARF} in CaP cells. ***A)*** Western blot analysis of p14^{ARF} in CaP cells. Both LNCaP (top panel) and 22Rv1 (bottom panel) cell lines were grown in 10% FBS media, and separately transfected with 50 nM of *miR-125b*, anti-*miR-125b*, miR-negative control (miR-NC) and anti-miR-negative control (anti-NC). Protein (50 μg) from cell lysates was electrophoresed on a 12% SDS-PAGE gel, and p14^{ARF} was detected with anti-p14^{ARF} antibody. The numbers under the gels are the fold changes of p14^{ARF} protein in *miR-125b*- or anti-*miR-125b*-treated cells relative to miR-NC or anti-NC-treated cells. Fold changes were calculated by scanning the p14^{ARF} bands and normalizing for β-actin bands. The data presented are representatives of three independent experiments. ***B***) p14^{ARF} level in *miR-125b* overexpressed mouse xenograft. Intact male nude mice were injected *s.c* with 2×10^6 lenti-*miR-125b*-PC-346C cells that overexpress *miR-125b*. Tumors were dissected 5 weeks after inoculation, and the level of p14^{ARF} was detected by Western blot analysis. ***C)*** Luciferase analysis of the 3'UTRs of *p14^{ARF}* in LNCaP cells. The 3'UTR of *p14^{ARF}* was cloned into a luciferase report vector in the 3' end of *LUC* gene. A truncated 3' UTR of *p14^{ARF}* without the *miR-125b* binding site was used as a control. The assay was repeated three times with each assay being performed in three wells and similar results were obtained each time. The representative results are shown as a mean ±SD (n=3).

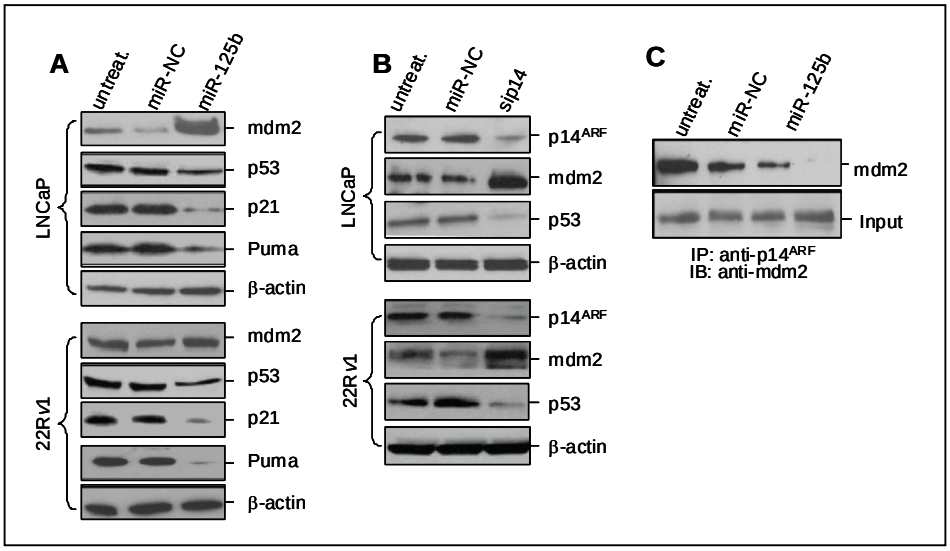

Figure 2: *MiR-125b*-p14^{ARF}signaling regulates the p53 network. ***A***) LNCaP (top panel) and 22Rv1 (bottom panel) cells were transfected with 50 nM of *miR-125b* or miR-NC. mdm2, p53, p21 and Puma were detected using individual specific antibodies. ***B***) Effect of *p14^{ARF}* siRNA (sip14) on the expression of p53 and mdm2. LNCaP (top panel) and 22Rv1 (bottom panel) cells were treated with sip14 and the expression levels of p14^{ARF}, p53 and mdm2 were analyzed by Western blotting analysis. ***C***) Effect of *miR-125b* on p14^{ARF}-mdm2

interaction. 22Rv1 cells were treated with *miR-125b*. Cell lysate was immuno-precipitated with $p14^{ARF}$ antibody and the control IgG. Co-IPed protein was probed with anti-mdm2 antibody.

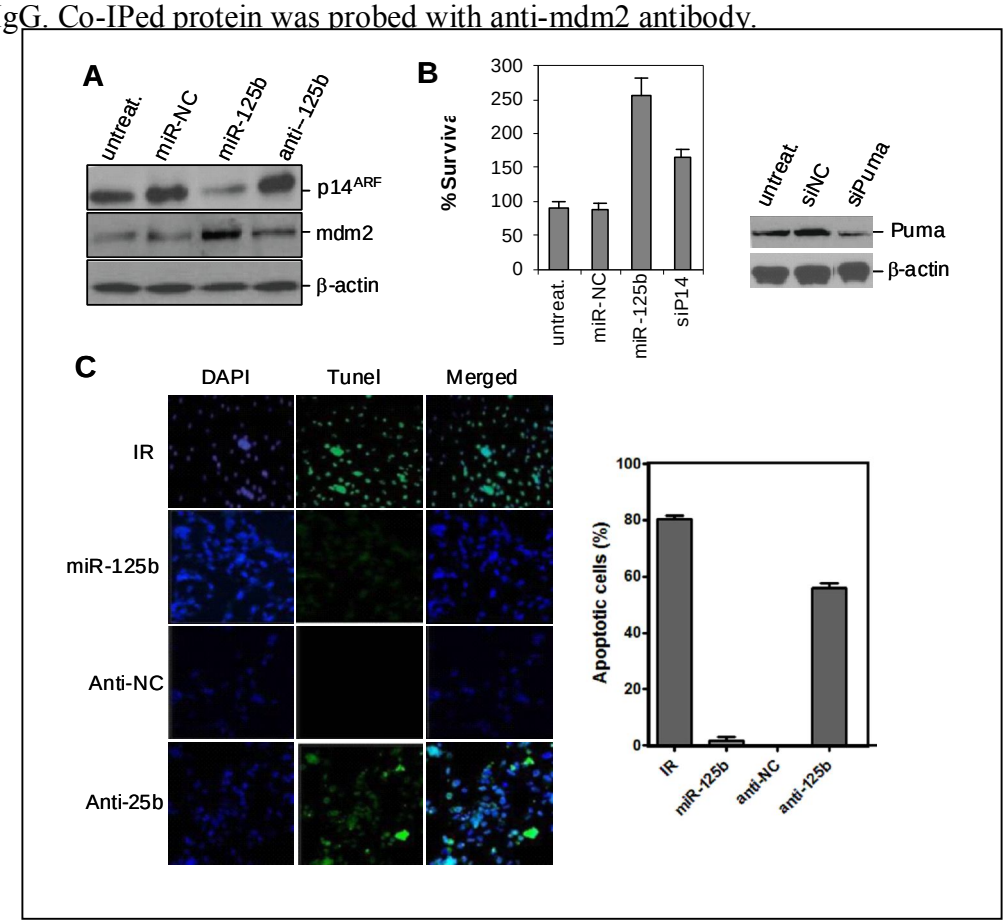

Figure3. Downregulation of *miR-125b* activity induces apoptosis in p53-null CaP cells. ***A***) Western blot analysis of $p14^{ARF}$ and mdm2 levels in p53-null PC3 cells transfected with *miR*-NC, *miR-125b* and *anti-125b*. ***B***) Effect of *miR-125b* on PC3 cell growth. PC3 cells were transfected first with siPuma followed by *miR-125b*. WST-1 proliferation assay was performed. Results are expressed as cell survival relative to that of untreated cells (100%). ***C***) Effects of anti-*miR-125b* on apoptosis. PC3 cells were transfected with anti-*miR-125b* and apoptotic death cells was detected by Tunel assay (left panel). The right panel shows quantitative apoptotic cell in treatment groups. Data represent the mean ± SE of 3 independent experiments.

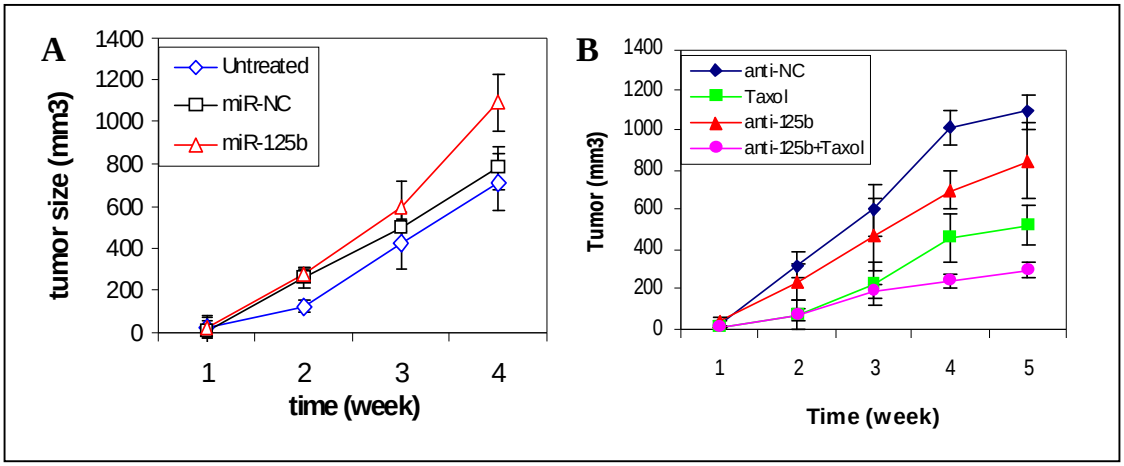

Figure 4. ***A***) *miR-125b* promotes growth of CWR22 xenografts. Intact male nude mice (8 per group) each were injected *s.c* with CWR22 cell suspensions. After inoculation, mice were immediately treated *i.v.* with polyethylenimines (PEI)-complexed *miR-125b* (10 μg/day, three times a week for 4 weeks) or miR-NC. ***B***)

Anti-*miR-125b* inhibits growth of CWR22 xenografts. Intact male nude mice bearing ~50 mm^3 CWR22 tumor were *i.v.* injected with PEI-complexed anti-*miR-125b* (10 μg/day, thrice a week for 4 weeks) or anti-*miR-125b* plus Taxol (20 mg/kg/week for 4 weeks). In these experiments, each time point represents mean ± SD of 8 independent values.

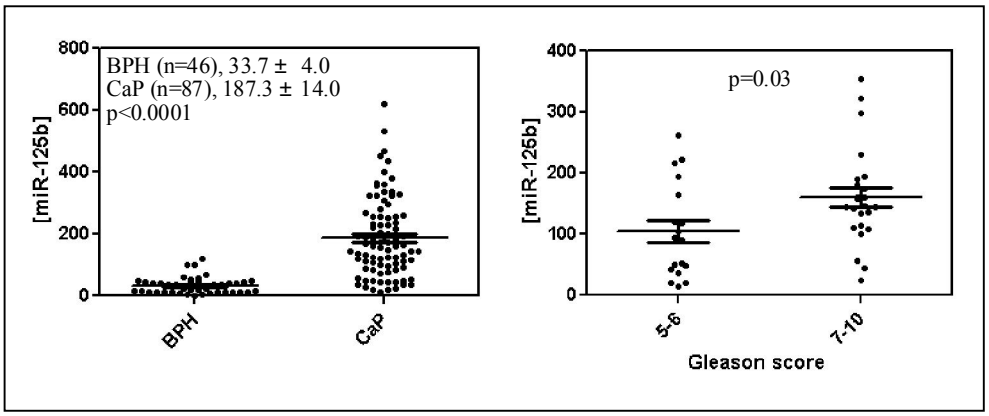

Figure 5. ***A***) Expression of *miR-125b in* clinical CaP tissues. The expression level of *miR-125b* was detected in 46 BPHs and 87 CaPs using qPCR. CaP samples express 3.0-fold greater elevation of *miR-125b* compared to BPHs. ***B***) 45 CaPs having known Gleason scores were divided two groups (Gleason score 5-6 and 7-10). A high level of *miR-125* was detected in patients with Gleason score 7-10 compared to that in Gleason score 5-6.

Tumor suppressive *miR-124* targets androgen receptor and inhibits proliferation of prostate cancer cells

Xu-Bao Shi[1], Lingru Xue[1], Ai-Hong Ma[2], Clifford G. Tepper[2], Regina Gandour-Edwards[3], Hsing-Jien Kung[2], Ralph W. deVere White[1¶].

[1]Department of Urology, [2]Department of Biochemistry and Molecular Medicine, and [3]Department of Pathology, University of California, Davis, School of Medicine, Sacramento, CA 95817, USA

Running title: *miR-124* and prostate cancer

Supported by NCI grant (CA92069) and DOD Grant (PC080488).

[¶]Address correspondence to: Department of Urology, University of California, Davis, School of Medicine 4860 Y Street, Suite 3500, Sacramento, California, 95817.

E-mail: rwdeverewhite@ucdavis.edu.

Abstract

Although prostate cancer (CaP) is the most frequently diagnosed malignant tumor in American men, the mechanisms underlying the development and progression of CaP remain largely unknown. Recent studies have shown that downregulation of *miR-124* occurs in several types of human cancer, suggesting a tumor suppressive function of *miR-124*. Until now, however, it has been unclear whether *miR-124* is associated with CaP. In the present study, we completed a series of experiments to understand the functional role of *miR-124* in CaP. We detected the expression level of *miR-124* in clinical CaP tissues, evaluated the influence of *miR-124* on the growth of CaP cells, and investigated the mechanism underlying the dysregulation of *miR-124*. We found that *i*) *miR-124* directly targets the androgen receptor (AR) and subsequently induces a upregulation of p53; *ii*) *miR-124* is significantly down-regulated in malignant prostatic cells compared to that in benign cells and DNA methylation causes the reduced expression of *miR-124*; and *iii*) *miR-124* can inhibit the growth of CaP cells *in vitro* and *in vivo*. Data from this study revealed that loss of *miR-124* expression is a common event in CaP, which may contribute to pathogenesis of CaP. Our studies also suggest that *miR-124* is a potential tumor suppressive gene in CaP, and restoration of *miR-124* expression may represent a novel strategy for CaP therapy.

Key Words: prostate cancer, androgen, androgen receptor, miRNA, tumor suppressor.

Introduction

Prostate cancer (CaP) is the most frequently diagnosed malignant tumor and was the second leading cause of cancer-related death in American men in 2011(Siegel et al 2012). Metastatic CaP can be treated effectively with androgen ablation. However, one of the most troubling aspects of this disease is that after hormone treatment, the tumor inevitably progresses from an androgen-dependent (AD) to an incurable castration-resistant (CR) form (Sadar 2011). The mechanism underlying the progression has been poorly understood. In the past decades, therefore, an important task in CaP research is to elucidate the molecular alteration occurring in the development of CR tumors. Considerable insight into the progression of CaP has been recently achieved, including the discovery of aberrantly expressed microRNAs (miRNAs).

The human genome may encode over 1000 miRNAs which negatively regulate approximately 60% of human genes (Friedman et al 2009, Lewis et al 2005). Thus, miRNAs are involved in almost all important cellular processes, not only in physiological conditions but also in diseases including cancer (Volinia et al 2006). Indeed, a number of cancer-related miRNAs have been identified recently. Some miRNAs have also been reported to be aberrantly expressed in human CaP (Shi et al 2008). These miRNAs, which act as tumor suppressor genes or oncogenes, contribute to the pathogenesis of CaP by directly targeting some proliferation-related genes or apoptotic molecules (Shenouda and Alahari 2009). In spite of these exciting findings, the role of miRNA in the development and progression of CaP has been largely unexplored. Thus, identifying CaP-associated miRNAs and investigating their roles in CaP will help us understand the mechanisms related to the development and progression of this disease.

MiR-124 is a highly conserved miRNA whose *in vivo* function is poorly defined. This small non-coding RNA was first reported to be highly expressed in neuronal cells (Makeyev et al 2007). Recent studies revealed that *miR-124* was significantly downregulated in several types of human cancers (Ando et al 2009, Furuta et al , Lujambio et al 2007). Moreover, it regulates some proliferation-related genes such as cyclin-dependent kinase 6 (CDK6) (Agirre et al 2009), forkhead box A2 (Foxa2) (Baroukh et al 2007) and solute carrier family 16, member 1 (SLC16A1) (Agirre et al 2009). Thus, *miR-124* is classified as tumor suppressor

miRNA (Agirre, 2009 #11). Until now, however, the role of *miR-124* in CaP has been totally unknown, although it was reported previously to be undetectable in 22Rv1 CaP cells (Mitchell et al 2008).

In the present study, we aimed to explore the role of *miR-124* in CaP. We found that *miR-124* directly targets the androgen receptor (AR). We also detected the expression level of *miR-124* in clinical CaP tissues and found that a majority of these CaP tissues express low levels of *miR-124*. In addition, we observed that synthetic *miR-124* mimics inhibit the proliferation of CaP cells. Since the AR plays a crucial role in the pathogenesis of CaP, our studies established a link between dysregulated *miR-124*, overexpressed AR and CaP cell proliferation. Our results imply that *miR-124* is a potential tumor suppressor gene and downregulation of *miR-124* contributes to the development and progression of CaP.

Results

***MiR-124* directly targets the AR and inhibits proliferation of CaP cells**. Overexpression of the AR is well known to play an important role in pathogenesis of CaP. We are very interested in determining whether certain miRNA(s) contribute to upregulation of the AR. From two algorithms, TargetScan (Release 5.2) and miRanda (August 2010 Release) that predict miRNA-binding sites in the first 436 base of the *AR* 3'UTR (NM_000044.2), we identified three broadly conserved miRNA-binding sites for six miRNAs (*miR-130/miR-301*, *miR-124/miR-506* and *miR-30*/*miR-384*). In order to assess the ability of these miRNAs to regulate AR expression, AR-positive C4-2B CaP cells cultured in androgen-deprived medium were separately treated with four chemically-modified miRNA mimics (*miR-124*, *miR-130*, *miR-384* or *miR-506*, purchased from Ambion). As shown in **Fig. 1A**, compared to miRNA negative control (miR-NC), treatment with *miR-124* mimic resulted in a reduction of AR protein by ~70%, while the other three miRNA mimics induced 20–40% decrease in AR expression, suggesting a potent downregulation of the AR by *miR-124*. To determine the influence of these miRNAs on proliferation of CaP cell, AR-positive CaP cell lines (LNCaP, C4-2B and 22Rv1) were transiently transfected with each of these miRNA mimics. Consistent with its effect on AR level, transfection of *miR-124* mimic inhibited proliferation to a greater extent than the other miRNA mimics tested (**SI Fig. 1**). We thus focused on *miR-124* in this study.

To determine whether *miR-124*-mediated downregulation of the AR affects the AR activity, both AR-positive LNCaP and C4-2B were treated with *miR-124* mimic. Western blot analysis demonstrated that *miR-124*-induced down-regulation of the AR and was concomitant with a reduced PSA level (**Fig. 1B**). Since AR regulates *miR-125b* (Shi et al 2007), we used C4-2B and cds2 cells which express increased *miR-125b* (Shi et al 2007) to examine the effect of *miR-124* mimic on endogenous *miR-125b*. We found that *miR-124* induced downregulation of *miR-125b* by 30% in C4-2B and 54% in cds2 (**Fig. 1C**). To verify that the putative *miR-124* binding site in the 3′ UTR of *AR* mRNA is responsible for regulation by *miR-124*, the 3′ UTR was cloned into a luciferase reporter vector and then cotransfected with *miR-124* mimic into C4-2B cells. Luciferase activity was measured two days after transfection. As shown in **Fig. 1D**, transfection of *miR-124* mimic resulted in 40% reduction of the enzyme activity, indicating a direct interaction between *miR-124* and *AR* mRNA. Taken together, these data indicate that *miR-124* targets the AR and affects the AR activity.

***MiR-124* is significantly downregulated in prostate cancer cells**. We determined the expression level of *miR-124* in CaP cells. The abundance of *miR-124* was first examined in seven prostate cell lines (2 benign and 5 malignant) using quantitative PCR (qPCR). We found a reduced expression of *miR-124* in the malignant lines compared to the benign lines (**Fig. 2A**). We also performed Northern blot analysis of these cell lines and similar results were obtained (**SI Fig. 2A).** Next, we tested whether *miR-124* is down-regulated in clinical prostate samples. We reviewed the miRNA expression profiling of our initial clinical tissue specimens and found that the abundance of *miR-124* is markedly reduced in four CaP samples relative to that in one benign prostatic hyperplasia (BPH) tissue (**SI Fig. 2B**). We then determined whether downregulation of *miR-124* is common in clinical CaP tissues. The levels of *miR-124* were detected in 79 clinical prostatic tissues including 19 BPHs, 44 primary CaPs, 6 lymph node metastases, and 10 CR tumors. Although *miR-124* abundances have overlap in a small number of benign and primary tumor tissues, the average *miR-124* level was 2.7-fold less in primary CaPs than in BPHs (39 in CaPs vs 146 in BPHs, $p<0.01$) (**Fig. 2B**). Interestingly, 10 CR tumors and 6 metastases expressed extremely low levels of *miR-124*.

Compared to the primary CaP samples, the averaged *miR-124* level decreases by 77% in these advanced tumors (39 in CaPs vs 9 in CR & metastatic tumors, $p<0.05$) (**Fig. 2B**), suggesting a potential involvement of *miR-124* in CaP progression. To confirm the downregulation of *miR-124*, 18 CaP samples and matched benign adjacent tissues were analyzed using qPCR. In comparison with matched benign tissues, 15 of 18 CaP samples (83%) expressed significantly reduced *miR-124* (**Fig. 2C**). In addition, we performed Northern blot analysis in five matched prostate tissues in which sufficient quantities of RNA were available. As expected, the three CaPs (8, 11 and 16) having low *miR-124* levels detected by qPCR exhibit lower signal intensity in Northern blots (**SI Fig. 2C**). Taken together, these data provide strong evidence that *miR-124* is significantly reduced in CaP cell lines and in a majority of clinical CaP samples, and also suggest that decreased expression of *miR-124* is common in human CaP tissues.

***MiR-124* and AR are negatively correlated in human CaP tissues.** Having demonstrated that *miR-124* targets the AR and is significantly downregulated in CaP cells, we therefore asked whether clinical CaP samples having low level of *miR-124* overexpressed the AR. To address the issue, eight additional matched pairs of CaP and BPH were examined for expression of AR protein using immunohistochemical (IHC) analysis. In these samples, *miR-124* level detected by qPCR was significantly decreased in CaP samples compared to that in BPH. Conversely, IHC results demonstrated that AR immunostaining was more intense in 7 of 8 CaP samples than that in BPH matches. These results reveal an inverse relationship between *miR-124* and AR expression levels in prostatic tissues. **Fig. 3** shows the representative results from four matches. In CaP samples AR protein staining is much higher than that in matched BPH tissues (**Fig. 3A**), while the expression of *miR-124* is significantly decreased in CaP tissue compared to that in BPH tissues (**Fig. 3B**). Therefore, our data suggest that down-regulation of *miR-124* results in increased expression of the AR in clinical CaP tissues.

***MiR-124* is methylated in CaP cells**. The question remained: why is *miR-124* downregulated in CaP cells? We first confirmed that androgens do not regulate *miR-124*, based on our observation that *miR-124* levels

were similar in androgen R1881-treated and untreated CaP cell lines (data not shown). Previous study has shown that DNA methylation regulates the expression of miRNAs (Sinkkonen et al 2008). Moreover, computer analysis demonstrated that the *miR-124-1* at 8p23.1 and the *miR-124-3* at 20q13.33 are embedded within CpG islands and the *miR-124-2* at 8q12.3 is 760 bp downstream of a CpG island (Agirre et al 2009). In order to determine that DNA methylation downregulates *miR-124* in CaP cells, we performed a demethylation experiment in three androgen-independent cell lines (22Rv1, C4-2B and cds2). Cells were treated with 50 μM of 5'-Aza-2'-Deoxycytidine (Aza) for 4 days and *miR-124* was detected by qPCR. It was found that Aza treatment induced 2- to 5-fold increase in the *miR-124* level compared to that in the untreated cells (**Fig. 4A**). Since *miR-124* targets the AR as shown in Figure 1, we tested whether Aza downregulates expression of the AR. It was found that treatment with Aza reduced the AR level by ~40% in LNCaP and ~ 60% in C4-2B cells (**Fig. 4B**). We then assessed the methylation status of two benign prostate cell lines (pRNS-1-1 and RWPE-1) and five CaP cell lines using methylation-specific PCR (MSP). The 5' DNA fragments of three *miR-124* genes were strongly amplified by MSP primers in all cell lines except RWPE-1 whose *miR-124-2* fragment was not amplified by the MSP primers (**Fig. 4C**). The fragments of *miR-124-1* and *miR-124-2* were also amplified weakly by unmethylated DNA primers in some of these cell lines (**Fig. 4C**). MSP data suggest different extents of DNA methylation at the 5' regions of *miR-124* genes. In order to validate DNA methylation, the 5' DNA fragments of three *miR-124* genes in six cell lines were amplified using COBRA (combined bisulfite restriction analysis) primers, cloned and sequenced. It was found that 40-80% of CpG sites were methylated in *miR-124-1*, 20-57% in *miR-124-2* and 15-31% in *miR-124-3*, in five CaP cell lines, and the CpG methylation are 18%, 13% and 8%, respectively, in benign RWPE-1 cells (**Fig. 4D**).

We next determined the methylation status in 9 BPH tissues and 14 CaP tissues using COBRA. The 5' DNA fragments of three *miR-124* genes that contain 2, 5 and 6 CGCG sites, respectively, were amplified with COBRA primers and digested with the restriction enzyme B*st*U1 which only cleaves methylated CGCG sites. It was found that B*st*U1 was able to cut the *miR-124-1* PCR products in 13 of 14 (93%) CaP samples, *miR-124-2* in 11 of 14 (79%) samples and *miR-124-3* in 12 of 14 (86%) samples, while the B*st*U1-digested

BPH DNA fragments of *miR-124* genes are 11% (1/9), 22% (2/9) and 44% (4/9), respectively (**Fig. 4E**), indicating that significant *miR-124* methylation occurs in clinical CaP specimens. Taken together, our data suggest that DNA methylation occurring at the 5' regions of *miR-124* genes causes, at least in part, the reduced expression of *miR-124* in CaP cells.

***MiR-124* induces apoptosis.** Previous studies demonstrated that the AR upregulates *miR-125b,* while *miR-125b* represses expression of p53 (Le et al 2009) and facilitates proliferation of CaP cells (Shi et al , Shi et al 2007). Since *miR-124* targets the AR and downregulates *miR-125b*, we asked whether increased *miR-124* level increases apoptotic cell death. To address the issue, LNCaP and C4-2B cells were transfected with *miR-124* mimic and then cultured for 4 days. Apoptotic death cells were quantitatively detected by Annexin V binding assay. We observed that *miR-124* mimic induced 10.4% of LNCaP cells and 9.7% of C4-2B cells to undergo apoptotic cell death (**Fig. 5A**). The comparative figure for the miR-NC cells was 0.7% and 1.1%, respectively ($p<0.01$). A representative Annexin V assay is shown in **SI Fig. 3** in which *miR-124* mimic-induced apoptosis (upper-right and lower-right squares in quadrant gates) were 11.4% of LNCaP cells and 8.4% of C4-2B cells. To provide biochemical evidence for the occurrence of apoptosis, we determined whether *miR-124* mimic increases the expression of p53 and caspase 3. As expected, treatment of C4-2B cells with *miR-124* mimic induced a ~9.0-fold enhanced expression of p53 (**Fig. 5B**) and ~2.0-fold increase in caspase 3 (**Fig. 5C**). These data indicate that *miR-124*, at least in part, induces apoptosis by activating the p53 signaling pathway.

***MiR-124* inhibits xenograft growth of CaP cells.** Having demonstrated that *miR-124* inhibits proliferation of AR-positive CaP cells and induces apoptosis, we tested whether this miRNA exerts an inhibitory effect on xenograft growth of CaP cells *in vivo*. We employed 22R*v*1 CaP cells to address this question due to their expression of low (Figure 2A) or undetectable (Mitchell et al 2008) level of *miR-124*, as well as their ability to efficiently form tumors in nude mice. Overexpression of *miR-124* in 22R*v*1 was established using lentiviral vector system that expresses 28-fold elevation of *miR-124* relative to controls (data not shown).

Xenograft tumors were generated by subcutaneously inoculating intact male nude mice with 22R*v*1-lenti-*miR-124* cells or 22R*v*1-lenti-vector cells. Tumors in *miR-124* group and control groups became palpable 18 days after inoculation, suggesting that *miR-124* did not affect the onset of 22R*v*1 tumor. However, overexpression of *miR-124* significantly inhibited the growth of 22R*v*1 tumors after three weeks when compared to controls (**Fig. 6A**). At the end of the experiments, qPCR analysisof *miR-124* level was performed in 3 lenti-*miR-124* tumors. It was found that *miR-124* levels were 23-fold increase in the *miR-124* tumors compared to the control tumors (**Fig. 6B**), similar to that in cultured 22R*v*1-lenti-*miR-124* cells, revealing a stable expression of *miR-124 in vivo*. In addition, one lenti-vector tumor and two lenti-*miR-124* tumors were examined by Western blot analysis for their AR expression. As shown in **Fig. 6C,** lenti-*miR-124* tumors express moderate reduction of the full-length AR. Interestingly, overexpression of *miR-124* in 22R*v*1 cells induced a downregulation of the truncated AR that may contribute to the aggressive features of 22R*v*1 cells (Tepper et al 2002). Collectively, our results suggest that *miR-124* inhibits growth of 22R*v*1 xenograft tumors by repressing AR expression.

Discussion

Although *miR-124* has been reported to be involved in several other cancer types (Ando et al 2009, Furuta et al , Lujambio et al 2007), its role in CaP is largely unknown. To date, only one study has reported that *miR-124* was undetectable in 22R*v*1 CaP cells (Mitchell et al 2008). The present study explored the role of *miR-124* in CaP. We found that *miR-124* directly targets the AR, suggesting a potential tumor suppressor gene in CaP. In addition, our expression analysis revealed that *miR-124* was significantly downregulated in a majority of clinical CaP specimens tested, which suggests that dysregulation of *miR-124* may be a common event in patients with CaP and loss of *miR-124* may contribute to the progression of CaP.

In this study, we address the potential mechanisms underlying *miR-124* down-regulation in CaP cells. Since methylation of tumor suppressor genes (TSGs) is very common in both early and advanced stages of CaP (Graff et al 1995, Kang et al 2004, Lou et al 1999, Woodson et al 2004), *miR-124* acting as a potential TSG in CaP may be susceptible to epigenetic modification. Indeed, we observed DNA methylation of three

miR-124 genes in CaP cell lines and clinical CaP samples, an explanation for the reduction of *miR-124* levels. This is supported by the fact that demethylation treatment with Aza increased the abundance of *miR-124* in CaP cells. These data provide strong evidence that *miR-124* is downregulated in CaP in part as a result of DNA methylation. Our results are consistent with those reported in other cancer types in which *miR-124* loci are aberrantly methylated (Agirre et al 2009, Furuta et al , Lujambio et al 2007). However, methylation of *miR-124* loci was not detected in a recent report (Rauhala et al 2010). In that study, Rauhala *et al.* treated CaP cells with 1 μM of Aza for two days followed by 300 nM of trichostatin A (TSA, a histone deacetylase inhibitor) for 24 hours. They identified 38 methylated miRNAs without *miR-124*. Mazar *et al* reported that Aza upregulates *miR-34b* expression in a dose-dependent manner and 1 μM of Aza did not induce elevation of *miR-34b* in melanoma cells (Mazar et al 2011). Since up to 100 μM of Aza failed to induce cytotoxicity in CaP cell lines (Walton et al 2008), we used 50 μM of Aza to treat CaP cells for four days, which induced significant elevation of *miR-124*. It is thus likely that our ability to detect the increased level of *miR-124* is due to the higher concentration of Aze used. Besides the epigenetic regulation, the expression level of *miR-124* can be affected by genetic factors, such as mutation and heterozygosity (LOH). Indeed, we detected a G→C point mutation (or SNP) in the 5' region of *miR-124-2* (**SI Fig. 4**). Mutation (or SNP) in 5' region can reduce expression of mature miRNA by altered miRNA processing (Davis and Hata 2009, Jazdzewski et al 2008). In addition, a previous study revealed that tumor suppressive miRNAs are frequently located in LOH regions (Calin et al 2004). We know that *miR-124-1* is located at 8p23.1 and *miR-124-2* at 8q12.3. LOH in these two regions were reported to occur in approximately 50% of CaPs (Chang et al 2007, Matsuyama et al 2003, Perinchery et al 1999). Thus, LOH may affect the levels of *miR-124-1 & miR-124-2.* In order to elucidate the mechanism underlying downregulation of *miR-124*, further study is needed to detect the frequencies of DNA mutation (or SNP) and LOH in three *miR-124* loci.

An interesting and clinically relevant discovery is that *miR-124* directly targets the AR. The AR contributes to the initiation and progression of CaP. A study has demonstrated that a moderately altered AR expression is sufficient to convert AD CaP cells to a CR form (Chen et al 2004). The AR has been reported to be upregulated in clinical CaPs, particularly those that are CR. Why AR is upregulated in CaP remains

poorly understood. *AR* gene amplification appears to account for the AR upregulation in ~30% CR CaPs (Koivisto et al 1997); however, it is unknown how the AR is upregulated in the other CR tumors. Since the 3'UTR of the *AR* mRNA contains a conserved *miR-124* binding site, we performed several experiments to validate the regulation of the AR by *miR-124*. We also observed an inverse correlation between *miR-124* abundance and the AR expression level in clinical CaP samples tested. Therefore, our study demonstrates that dysregulation of *miR-124* may elevate the expression of the AR, which is a new mechanistic explanation for overexpression of the AR in CaP. In this present study, identification of *miR-124* as AR-targeting miRNA was based on the TargetScan and miRanda prediction programs. We noted that *miR-124*, as well as other three predicted miRNAs as shown in Figure 1A, were not selected as AR-targeting miRNAs in a recent study (Ostling et al 2011). In that study, the authors transfected five AR-positive CaP cell lines with 20 nM of human miRNA library and selected 71 miRNA candidates that affect the level of AR in all five cell lines. However, miRNA repression of target molecular expression is dose-dependent (Yamakuchi et al 2008). The dose of *miR-124* mimic used in this study is 100 nM. In addition, miRNA functions in a cell type- and context-dependent manner (Olive et al 2010), and some AR-targeting miRNAs may not equally affect the AR level in all five CaP cell lines. Therefore, different treatment conditions and different selection criteria may account for the differential results.

Although we focus on the AR in this study, we realize that *miR-124* targets hundreds of human genes, and other potential targets may also be relevant for the tumor suppressive function of *miR-124* in CaP. We have identified a putative *miR-124* binding site in the 3'UTR of high mobility group AT-hook 1 gene (*HMGA1*). In a pilot study, transfection of C4-2B cells with *miR-124* mimic resulted in reduction of HMGA1 expression by 60%; furthermore, two clinical CaP specimens having low level of *miR-124* did overexpress cytoplasmic HMGA1 (see **SI Fig. 5**), suggesting a link between low *miR-124* and overexpression of HMGA1 in CaP. Previous studies revealed that HMGA1 was highly expressed in advanced CaPs (Takaha et al 2002, Tamimi et al 1993), and cytoplasmic HMGA1 directly interacts with p53, leading to p53 inactivation (Frasca et al 2006, Pierantoni et al 2006). Therefore, functional characterization of this *miR-124* target will provide new insight into elucidating the molecular alteration occurring in advanced CaP.

Additionally, cyclin-dependent kinase 6 (CDK6) and forkhead box A2 (Foxa2) have been identified as promising targets of *miR-124* (Agirre et al 2009, Baroukh et al 2007). Both CDK6 and Foxa2 were previously reported to be elevated in CaP cells and correlate with tumor grade (Chen et al 1996, Mirosevich et al 2006, Qi et al). Moreover, these two proteins interact with the AR and enhance the AR activity (Lim et al 2005, Yu et al 2005). Further studies are required to understand whether upregulation of these two molecules in CaP cells are the result of decreased expression of *miR-124*.

Consistent with a previous report in nerve cells (Cao et al 2007), restoration of *miR-124* level by transfecting CaP cells with synthetic *miR-124* induces increased apoptosis. We also found that treatment of CaP cells with *miR-124* upregulated the expression of p53, which is due at least partially to *miR-124*-mediated inhibition of AR/*miR-125b* signaling (Shi et al 2007). Thus, upregulation of p53 signaling may play a key role in *miR-124*-induced apoptosis. Since *miR-124* induces apoptosis, we evaluated its effect on proliferation of CaP cells. Restoration of *miR-124* level significantly inhibited the growth of CaP cells. More interestingly, when lentiviral-transduced 22Rv1 CaP cells that stably express *miR-124* were injected subcutaneously into intact male nude mice, xenograft tumor growth also was significantly inhibited. Therefore, further testing of *miR-124* in pre-clinical models of CaP will help define its ultimate therapeutic potential for treatment of CaP.

In conclusion, this study has shown that loss of *miR-124* expression may be a common event in CaP. Since *miR-124* negatively regulates the AR, downregulation of *miR-124*, as found in CaP, increases expression of the receptor. Therefore, deregulation of *miR-124* as well as other AR-targeting miRNA candidates (Ostling et al 2011) contributes to high levels of AR expression in clinical CaP. Additionally, our data suggest that downregulation of *miR-124* may be involved in the pathogenesis of CaP. Our evidence supporting the ability of *miR-124* to induce apoptosis in CaP cells encourages the hope that restoring *miR-124* function in CaP cells, either by itself or in conjunction with other therapies, will offer improved survival, which will be through delayed development or treatment of CR prostate cancer.

Materials and Methods

Cell lines: Two immortalized benign prostatic epithelial cell lines (RWPE-1 and pRNS-1-1) and five CaP cell lines (LNCaP, C4-2B, cds2, 22R*v*1 and LAPC-4) were employed in this study. RWPE-1 (provided by Dr. Mukta. Webber, Michigan State University, East Lansing, MI) and pRNS-1-1 (provided by Dr. Johng Rhim, University of the Health Sciences, Bethesda, MD) were maintained in keratinocyte serum-free medium supplemented with 50 mg/ml bovine pituitary extract and 5 ng/ml epidermal growth factor. CaP cell lines were maintained in RPMI 1640 medium containing 10% fetal bovine serum. Both C4-2B and cds2 cell lines are derivatives of LNCaP (Lin et al 2001, Shi et al 2004).

Clinical samples. Collection and use of CaP patient specimens were approved by the Institutional Review Board (UCD IRB#: 200312072-6). Primary CaP samples from radical prostatectomy, metastatic pelvic lymph nodes, CR tumor specimens and BPH tissues were obtained fresh from surgical excision by the Department of Urology, University of California, Davis. These CR tumors were described in our previous publication (de Vere White et al 1997): six from stage D patients and four from patients receiving combined androgen blockade therapy prior to radical prostatectomy. To ensure that portions of CaP tissues were enriched for tumor cells, a surgeon and a pathologist together sectioned the excised tissue, and a fresh piece was taken from the palpated cancer and rapidly frozen to -80^{o}C until use. A permanent section was then cut from the immediately adjacent area for Hematoxylin and Eosin (H&E) staining. Based upon histological review of H&E section, it was confirmed that these CaP samples used in this study were tumor cell-enriched.

Reporter plasmid construction and luciferase assay. To construct reporter plasmids, a 0.45-kb DNA fragment of the *AR* 3′UTR containing the putative *miR-124* binding site was prepared by PCR. The *AR* 3′UTR fragment lacking the *miR-124* binding site was used as negative control. DNA fragments were cloned into the pMIR-REPORT Luciferase vector (Ambion) downstream of the reporter gene. The sequences and cloning direction of these PCR products were validated by DNA sequencing. For luciferase assay, cells (4×10^4 per well) were seeded into 24-well plates and cultured for 24 hours. The cells were then co-transfected with reporter plasmids and 100 nM chemically-modified *miR-124* mimic or miRNA negative

control (miR-NC). The pRL-SV40 Renilla luciferase plasmid (Promega) was used as an internal control. Two days later, cells were harvested and lysed with passive lysis buffer (Promega). Luciferase activity was measured using a dual luciferase reporter assay (Promega). Luciferase activity was normalized by Renilla luciferase activity.

Western blot analysis. Cells were grown to 70–80% confluence and lysed in lysis buffer consisting of 25 mmol/L Tris-HCl (pH7.5), 150 mmol/L NaCl, 1 mmol/L EDTA, 1% Triton X-100, 0.1% SDS and 1× proteinase inhibitor cocktail, and equal concentrations of denatured protein samples were loaded on a 10% SDS–polyacrylamide gel. After electrophoresis, proteins were transferred to an Immobilon PVDF membrane, and immunoblot analysis was conducted by the standard method.

qPCR. For quantitative expression analysis of miRNA, total RNA was isolated from fresh-frozen prostatic tissues, cultured cells or xenograft tumors using TRIzol reagent (Life Technologies, Inc.). The miRNA level was measured using a TaqMan miRNA assay kit (Applied Biosystems, Foster City, CA) following the manufacturer's instruction and PCR amplification was carried out in a 7900HT Fast Real-time PCR system (Applied Biosystems). Real-time PCR was performed in triplicate for each sample. The abundance of miRNA was measured using C_t (threshold cycle) following the approach described previously (Schmittgen and Livak 2008). ΔC_t was calculated by subtracting the C_t of *U6* RNA from the C_t of the miRNA tested. $\Delta\Delta C_t$ was calculated by subtracting the ΔC_t of a reference sample from the ΔC_t of each sample. For clinical tissues, the reference sample is one CaP specimen tested that expresses the lowest level of miRNA. Fold change was generated using the equation $2^{-\Delta\Delta Ct}$.

Methylation assay. Genomic DNA was isolated from prostate cell lines using standard procedures, and from CaP cell-enriched tumor tissues following our previous method (Shi et al 1996). Bisulfite modification of DNA (1.0 μg) was carried out by using an EZ DNA methylation-direct kit (Zymo Research, Irvine, CA). For the prostate cell lines, the methylation of 5' CpG island regions was detected by MSP using the primers

specific for either methylated or unmethylated DNA. The methylated CpG dinucleotides were validated using bisulfite DNA sequencing. Amplified CpG islands were separately cloned into pCR 2.1 vector using TOPO TA Cloning Kit (Invitrogen) and at least three clones per PCR product were picked up for DNA sequencing. In clinical prostate tissues, the methylation status was assessed by COBRA assay. COBRA primer-amplified PCR products were purified using Amicon 30 filter (Millipore), digested by BstUI and separated on a 3% agarose gel (1% agarose plus 2% NuSieve GTG low-melting temperature agaros). The primers used for MSP and COBRA were designed based on "The Li Lab" program (http://www.urogene.org/methprimer/index1.html). The primer sequences and amplified size are listed in **SI Table 1.**

Annexin V binding assay. *MiR-124*-induced apoptosis was analyzed using a FACS Annexin V assay kit (Trevigen, Inc., Gaithersburg, MD) following the protocol provided by the manufacturer. Briefly, cells were transfected with *miR-124* mimic and incubated for 4 days. The cells were harvested, washed once with PBS, re-suspended in 100 µl of 1× Annexin V binding buffer containing 1 µl of Annexin V-FITC conjugate and 10 µl of propidium iodide solution and then incubated for 30 min at room temperature in the dark. Subsequently, 400 µl 1× Annexin V binding buffer was added and samples analyzed on a FACScan flow cytometer. Data analysis was performed using FACScan software (Becton Dickinson).

Animal experiment. A lentiviral *miR-124* expression vector that expresses a ~500-base human pre-*miR-124*-1 and the empty lentiviral vector were purchased from System Biosciences (SBI, Mountain View, CA). Pseudovirus production and cell transduction were performed following the manufacturer's protocol. The resulting 22R*v*1-*miR-124* and 22R*v*1-vector cells were selected through fluorescence-activated cell sorting (FACS) and were maintained in medium described above. Overexpression of *miR-124* in infected 22R*v*1 cells was confirmed by qPCR. Animal studies were performed in male athymic nu/nu mice (4- to 6-week-old; Harlan Laboratories). Mice were injected subcutaneously with suspensions of 2×10^6 22R*v*1-*miR-124* cells or 22R*v*1-vector cells in a mixture (1:1 vol/vol) of culture medium and Matrigel (Becton Dickinson).

Tumor growth was monitored and tumor dimensions were measured twice per week. Tumor volumes were calculated according to the formula: ½ (length×width×height). Animal studies were performed according to protocols approved by the Animal Care and Use Committee at University of California, Davis.

Statistical analysis. Statistical analysis was performed using GraphPad Prism software 5.0. Student's t-test was used to analyze the difference in *miR-124* levels between different groups. Statistical significance was set up to $p<0.05$ in each test.

Conflict of interest

The authors declare no conflict of interest.

Acknowledgments

This work was supported in part by NIH 1RO1CA92068 (R. deVere White), Department of Defense PCRP PC080488 (R. deVere White) and The LANIE Foundation. We thank Dr. Mukta. Webber for providing RWPE-1 cell line and Dr. Johng Rhim for pRNS-1-1 cell line. We also gratefully thank Dr. Melanie C. Bradnam for her editorial assistance and Stephanie Soares for critically reading the manuscript.

References

Agirre X, Vilas-Zornoza A, Jimenez-Velasco A, Martin-Subero JI, Cordeu L, Garate L *et al* (2009). Epigenetic silencing of the tumor suppressor microRNA Hsa-miR-124a regulates CDK6 expression and confers a poor prognosis in acute lymphoblastic leukemia. *Cancer Res* **69:** 4443-4453.

Ando T, Yoshida T, Enomoto S, Asada K, Tatematsu M, Ichinose M *et al* (2009). DNA methylation of microRNA genes in gastric mucosae of gastric cancer patients: its possible involvement in the formation of epigenetic field defect. *Int J Cancer* **124:** 2367-2374.

Baroukh N, Ravier MA, Loder MK, Hill EV, Bounacer A, Scharfmann R *et al* (2007). MicroRNA-124a regulates Foxa2 expression and intracellular signaling in pancreatic beta-cell lines. *J Biol Chem* **282:** 19575-19588.

Calin GA, Sevignani C, Dumitru CD, Hyslop T, Noch E, Yendamuri S *et al* (2004). Human microRNA genes are frequently located at fragile sites and genomic regions involved in cancers. *Proc Natl Acad Sci U S A* **101:** 2999-3004.

Cao X, Pfaff SL, Gage FH (2007). A functional study of miR-124 in the developing neural tube. *Genes Dev* **21:** 531-536.

Chang BL, Liu W, Sun J, Dimitrov L, Li T, Turner AR *et al* (2007). Integration of somatic deletion analysis of prostate cancers and germline linkage analysis of prostate cancer families reveals two small consensus regions for prostate cancer genes at 8p. *Cancer Res* **67:** 4098-4103.

Chen CD, Welsbie DS, Tran C, Baek SH, Chen R, Vessella R *et al* (2004). Molecular determinants of resistance to antiandrogen therapy. *Nat Med* **10:** 33-39.

Chen Y, Robles AI, Martinez LA, Liu F, Gimenez-Conti IB, Conti CJ (1996). Expression of G1 cyclins, cyclin-dependent kinases, and cyclin-dependent kinase inhibitors in androgen-induced prostate proliferation in castrated rats. *Cell Growth Differ* **7:** 1571-1578.

Davis BN, Hata A (2009). Regulation of MicroRNA Biogenesis: A miRiad of mechanisms. *Cell Commun Signal* **7:** 18.

de Vere White R, Meyers F, Chi SG, Chamberlain S, Siders D, Lee F *et al* (1997). Human androgen receptor expression in prostate cancer following androgen ablation. *European urology* **31:** 1-6.

Frasca F, Rustighi A, Malaguarnera R, Altamura S, Vigneri P, Del Sal G *et al* (2006). HMGA1 inhibits the function of p53 family members in thyroid cancer cells. *Cancer Res* **66:** 2980-2989.

Friedman RC, Farh KK, Burge CB, Bartel DP (2009). Most mammalian mRNAs are conserved targets of microRNAs. *Genome Res* **19:** 92-105.

Furuta M, Kozaki KI, Tanaka S, Arii S, Imoto I, Inazawa J miR-124 and miR-203 are epigenetically silenced tumor-suppressive microRNAs in hepatocellular carcinoma. *Carcinogenesis* **31:** 766-776.

Graff JR, Herman JG, Lapidus RG, Chopra H, Xu R, Jarrard DF *et al* (1995). E-cadherin expression is silenced by DNA hypermethylation in human breast and prostate carcinomas. *Cancer Res* **55:** 5195-5199.

Jazdzewski K, Murray EL, Franssila K, Jarzab B, Schoenberg DR, de la Chapelle A (2008). Common SNP in pre-miR-146a decreases mature miR expression and predisposes to papillary thyroid carcinoma. *Proc Natl Acad Sci U S A* **105:** 7269-7274.

Kang GH, Lee S, Lee HJ, Hwang KS (2004). Aberrant CpG island hypermethylation of multiple genes in prostate cancer and prostatic intraepithelial neoplasia. *J Pathol* **202:** 233-240.

Koivisto P, Kononen J, Palmberg C, Tammela T, Hyytinen E, Isola J *et al* (1997). Androgen receptor gene amplification: a possible molecular mechanism for androgen deprivation therapy failure in prostate cancer. *Cancer Res* **57:** 314-319.

Le MT, Teh C, Shyh-Chang N, Xie H, Zhou B, Korzh V *et al* (2009). MicroRNA-125b is a novel negative regulator of p53. *Genes Dev* **23:** 862-876.

Lewis BP, Burge CB, Bartel DP (2005). Conserved seed pairing, often flanked by adenosines, indicates that thousands of human genes are microRNA targets. *Cell* **120:** 15-20.

Lim JT, Mansukhani M, Weinstein IB (2005). Cyclin-dependent kinase 6 associates with the androgen receptor and enhances its transcriptional activity in prostate cancer cells. *Proc Natl Acad Sci U S A* **102:** 5156-5161.

Lin DL, Tarnowski CP, Zhang J, Dai J, Rohn E, Patel AH *et al* (2001). Bone metastatic LNCaP-derivative C4-2B prostate cancer cell line mineralizes in vitro. *Prostate* **47:** 212-221.

Lou W, Krill D, Dhir R, Becich MJ, Dong JT, Frierson HF, Jr. *et al* (1999). Methylation of the CD44 metastasis suppressor gene in human prostate cancer. *Cancer Res* **59:** 2329-2331.

Lujambio A, Ropero S, Ballestar E, Fraga MF, Cerrato C, Setien F *et al* (2007). Genetic unmasking of an epigenetically silenced microRNA in human cancer cells. *Cancer Res* **67:** 1424-1429.

Makeyev EV, Zhang J, Carrasco MA, Maniatis T (2007). The MicroRNA miR-124 promotes neuronal differentiation by triggering brain-specific alternative pre-mRNA splicing. *Mol Cell* **27:** 435-448.

Matsuyama H, Pan Y, Yoshihiro S, Kudren D, Naito K, Bergerheim US *et al* (2003). Clinical significance of chromosome 8p, 10q, and 16q deletions in prostate cancer. *Prostate* **54:** 103-111.

Mazar J, Khaitan D, DeBlasio D, Zhong C, Govindarajan SS, Kopanathi S *et al* (2011). Epigenetic regulation of microRNA genes and the role of miR-34b in cell invasion and motility in human melanoma. *PloS one* **6:** e24922.

Mirosevich J, Gao N, Gupta A, Shappell SB, Jove R, Matusik RJ (2006). Expression and role of Foxa proteins in prostate cancer. *Prostate* **66:** 1013-1028.

Mitchell PS, Parkin RK, Kroh EM, Fritz BR, Wyman SK, Pogosova-Agadjanyan EL *et al* (2008). Circulating microRNAs as stable blood-based markers for cancer detection. *Proc Natl Acad Sci U S A* **105:** 10513-10518.

Olive V, Jiang I, He L (2010). mir-17-92, a cluster of miRNAs in the midst of the cancer network. *The international journal of biochemistry & cell biology* **42:** 1348-1354.

Ostling P, Leivonen SK, Aakula A, Kohonen P, Makela R, Hagman Z *et al* (2011). Systematic analysis of microRNAs targeting the androgen receptor in prostate cancer cells. *Cancer Res* **71:** 1956-1967.

Perinchery G, Bukurov N, Nakajima K, Chang J, Hooda M, Oh BR *et al* (1999). Loss of two new loci on chromosome 8 (8p23 and 8q12-13) in human prostate cancer. *Int J Oncol* **14:** 495-500.

Pierantoni GM, Rinaldo C, Esposito F, Mottolese M, Soddu S, Fusco A (2006). High Mobility Group A1 (HMGA1) proteins interact with p53 and inhibit its apoptotic activity. *Cell Death Differ* **13:** 1554-1563.

Qi J, Nakayama K, Cardiff RD, Borowsky AD, Kaul K, Williams R *et al* Siah2-dependent concerted activity of HIF and FoxA2 regulates formation of neuroendocrine phenotype and neuroendocrine prostate tumors. *Cancer Cell* **18:** 23-38.

Rauhala HE, Jalava SE, Isotalo J, Bracken H, Lehmusvaara S, Tammela TL *et al* (2010). miR-193b is an epigenetically regulated putative tumor suppressor in prostate cancer. *Int J Cancer* **127:** 1363-1372.

Sadar MD (2011). Small molecule inhibitors targeting the "achilles' heel" of androgen receptor activity. *Cancer Res* **71:** 1208-1213.

Schmittgen TD, Livak KJ (2008). Analyzing real-time PCR data by the comparative C(T) method. *Nat Protoc* **3:** 1101-1108.

Shenouda SK, Alahari SK (2009). MicroRNA function in cancer: oncogene or a tumor suppressor? *Cancer Metastasis Rev* **28:** 369-378.

Shi XB, Xue L, Ma AH, Tepper CG, Kung HJ, White RW miR-125b promotes growth of prostate cancer xenograft tumor through targeting pro-apoptotic genes. *Prostate* **71:** 538-549.

Shi XB, Bodner SM, deVere White RW, Gumerlock PH (1996). Identification of p53 mutations in archival prostate tumors. Sensitivity of an optimized single-strand conformational polymorphism (SSCP) assay. *Diagn Mol Pathol* **5:** 271-278.

Shi XB, Ma AH, Tepper CG, Xia L, Gregg JP, Gandour-Edwards R *et al* (2004). Molecular alterations associated with LNCaP cell progression to androgen independence. *Prostate* **60:** 257-271.

Shi XB, Xue L, Yang J, Ma AH, Zhao J, Xu M *et al* (2007). An androgen-regulated miRNA suppresses Bak1 expression and induces androgen-independent growth of prostate cancer cells. *Proc Natl Acad Sci U S A* **104:** 19983-19988.

Shi XB, Tepper CG, White RW (2008). MicroRNAs and prostate cancer. *J Cell Mol Med* **12:** 1456-1465.

Siegel R, Ward E, Brawley O, Jemal A (2012). Cancer statistics, 2011: the impact of eliminating socioeconomic and racial disparities on premature cancer deaths. *CA Cancer J Clin* **61:** 212-236.

Sinkkonen L, Hugenschmidt T, Berninger P, Gaidatzis D, Mohn F, Artus-Revel CG *et al* (2008). MicroRNAs control de novo DNA methylation through regulation of transcriptional repressors in mouse embryonic stem cells. *Nat Struct Mol Biol* **15:** 259-267.

Takaha N, Hawkins AL, Griffin CA, Isaacs WB, Coffey DS (2002). High mobility group protein I(Y): a candidate architectural protein for chromosomal rearrangements in prostate cancer cells. *Cancer Res* **62:** 647-651.

Tamimi Y, van der Poel HG, Denyn MM, Umbas R, Karthaus HF, Debruyne FM *et al* (1993). Increased expression of high mobility group protein I(Y) in high grade prostatic cancer determined by in situ hybridization. *Cancer Res* **53:** 5512-5516.

Tepper CG, Boucher DL, Ryan PE, Ma AH, Xia L, Lee LF *et al* (2002). Characterization of a novel androgen receptor mutation in a relapsed CWR22 prostate cancer xenograft and cell line. *Cancer Res* **62:** 6606-6614.

Volinia S, Calin GA, Liu CG, Ambs S, Cimmino A, Petrocca F *et al* (2006). A microRNA expression signature of human solid tumors defines cancer gene targets. *Proc Natl Acad Sci U S A* **103:** 2257-2261.

Walton TJ, Li G, Seth R, McArdle SE, Bishop MC, Rees RC (2008). DNA demethylation and histone deacetylation inhibition co-operate to re-express estrogen receptor beta and induce apoptosis in prostate cancer cell-lines. *Prostate* **68:** 210-222.

Woodson K, Hanson J, Tangrea J (2004). A survey of gene-specific methylation in human prostate cancer among black and white men. *Cancer Lett* **205:** 181-188.

Yamakuchi M, Ferlito M, Lowenstein CJ (2008). miR-34a repression of SIRT1 regulates apoptosis. *Proc Natl Acad Sci U S A* **105:** 13421-13426.

Yu X, Gupta A, Wang Y, Suzuki K, Mirosevich J, Orgebin-Crist MC *et al* (2005). Foxa1 and Foxa2 interact with the androgen receptor to regulate prostate and epididymal genes differentially. *Ann N Y Acad Sci* **1061:** 77-93.

Legends

Figure 1. *MiR-124* negatively regulates androgen receptor (AR). ***A***) Western blot analysis of the AR expression in C4-2B CaP cells that were treated with 100 nM of synthetic *miR-124*, *miR-130*, *miR-384* or *miR-506*. The numbers under the gels are the fold changes of AR protein relative to untreated C4-2B cells (untreat.). Fold changes were calculated by scanning the AR bands and normalizing for β-actin bands. The upper portion is a schema of the first 436 bases of the *AR* 3′ UTR (based on the RefSeq NM_000044.2). The digital numbers indicate the predicted three miRNA-binding sites targeted by six potential AR-targeting miRNAs. ***B***) Western blot analysis of the expression of AR and PSA in LNCaP and C4-2B cells treated with 100 nM of *miR-124* mimic. Both mock and miRNA-NC were used as controls. ***C***) Quantitative PCR (qPCR) assay of *miR-125b* levels in C4-2B and cds2 cells treated with 100 nM of *miR-124* mimic or miR-NC. The values shown as mean ± SE (n=3) are from three independent experiments performed in triplicate. ***D***) Luciferase analysis in C4-2B cells. The assay was repeated three times with each assay being performed in four wells, and similar results were obtained each time. The representative results are shown as mean ± SD (n = 4). The percentage represents enzyme activity in 100 nM *miR-124* mimic-transfected cells relative to that in 100 nM miR-NC-transfected cells. RLU, relative luciferase unit. ΔBS3'UTR, AR 3′UTR fragment lacking the *miR-124* binding site.

Figure 2. Quantitative PCR (qPCR) assays of *miR-124* expression levels in CaP cells. ***A***) *MiR-124* abundance in two benign prostate cell lines (pRNS-1-1 and RWPE-1) and five CaP cell lines (22R*v*1, LNCaP, LAPC-4, cds2 and C4-2B). ***B***) *MiR-124* expression levels in 19 benign prostatic hyperplasia (BPH) tissues, 44 primary CaPs, 6 lymph node metastases and 10 castration-resistant tumors. ***C***) *MiR-124* levels in 18 matched benign and malignant prostate samples. The levels of *miR-124* of five pairs of prostate tissues (5, 8, 9, 11 & 16) were assayed using Northern blot analysis and similar results were obtained. The Northern blot results are shown in SI Figure 2B. "*", no statistical difference ($p>0.05$) between BPH and CaP tissues. In ***A***, ***B*** and ***C***, qPCR assays were repeated three times with each assay being performed in triplicate, and similar results were obtained each time. The values are shown as mean ± SE (n=3).

Figure 3. The expression levels of androgen receptor (AR) and *miR-124* in four matched prostate tissues (pt-1 to pt-4). ***A***) Immunohistochemical analysis of the AR protein in four human CaP samples (*right*) and their benign prostate tissue (*left*). ***B***) qPCR detection of the abundance of *miR-124* in both BPH and CaP tissues. The values are shown as mean ± SE from three independent experiments.

Figure 4. Methylation of *miR-124* in CaP cells. ***A***) Expression levels of *miR-124* in 22R*v*1, C4-2B and cds2 CaP cell lines before and after treatment with 50 μM of Aza. Results are expressed as fold change of *miR-124* relative to the untreated control. The assay was repeated three times with each assay being performed in three wells, and similar results were obtained each time. The representative results are shown as mean ± SD (n = 3). ***B***) Western blot analysis of the AR expression in LNCaP and C4-2B cells treated with 50 μM of Aza. ***C***) Methylation-specific PCR (MSP) assay of the 5' CpG islands of *miR-124-1*, *miR-124-2* and *miR-124-3* in seven prostatic cell lines: two benign lines (pRNS-1-1 and RWPE-1) and 5 malignant lines (22R*v*1, LNCaP, LAPC-4, cds2 and C4-2B). ***D***) Bisulfite sequencing analysis of *miR-124* CpG island methylation in RWPE-1 cell line and five CaP cell lines. The top schematic view represents individual amplified 5' DNA fragments of three *miR-124* genes, which are located at -1895 to -1655 upstream of pre-*miR-124-1*, -1456 to -1188 of pre-*miR-124-2* and -1465 to -1246 of pre-*miR-124-3*. The vertical bars denote individual CpG dinucleotides. Methylation profiles of *miR-124* CpG island fragments in six cell lines tested were demonstrated in the bottom of the schema. CpGs are represented by open circles if unmethylated and by black circles if methylated. Each row exhibits methylated CpGs from at least three clones. The numbers on the right of each row are the percentage of methylated CpG dinucleotides. ***E***) COBRA analysis of methylation of *miR-124-1*, *miR-124-2* and *miR-124-3* in 9 BPH tissues and 14 CaP samples. Purified PCR product was digested with B*st*UI that cuts methylated CGCG. The black arrows indicate the BPH samples having detectable methylation, and the white arrows indicate the CaP samples without methylation.

Figure 5. *MiR-124* induces apoptosis and upregulates p53. ***A***) Annexin V assay of apoptosis. LNCaP and C4-2B cells were treated with 100 nM *miR-124* mimic or miR-NC for 4 days and stained with Annexin V and propidium iodide. Both early and late apoptotic cells are combined. The values are shown as mean ± SE from three independent experiments. ***B***) Western blotting analysis of p53 expression in 100 nM *miR-124* mimic-transfectd C4-2B cells. Doxorubicin (Dox)-treated cells were used as positive control. ***C***) Western blotting analysis of caspase 3 (Cas-3) in 100 nM *miR-124* mimic-transfectd C4-2B cells. In both ***B*** and ***C,*** the numbers under the gels are the fold changes of p53 and Cas-3 in *miR-124* mimic-treated C4-2B cells relative to miR-NC-treated cells.

Figure 6. Inhibition of xenograftic tumor growth by *miR-124*. ***A***). Five nude mice per group were injected subcutaneously with 2×10^6 22R*v*1-*miR-124* cells, 22R*v*1-vector cells, or untreated 22R*v*1 cells. The growth of xenograft tumors were measured twice per week. Each time point represents mean ± SD of five independent values (mm^3). ***B***) qPCR assay of *miR-124* level in xenograft tumors. The assay was repeated twice and similar results were obtained each time. The representative results are shown as mean ± SD (n = 3). ***C***) Western blot assay of the AR expression in two 22R*v*1-*miR-124* tumors that express the full-length AR and a truncated AR (Tepper et al 2002).

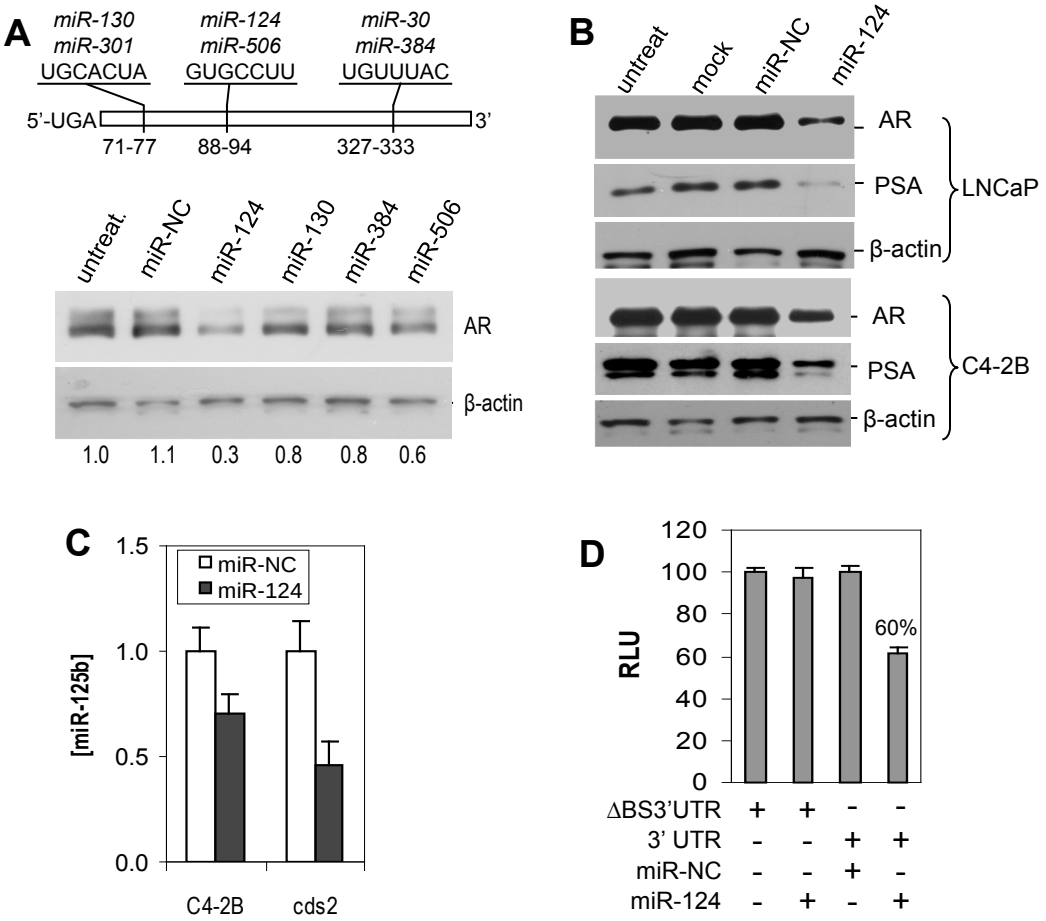
A
miR-130
miR-301
UGCACUA
miR-124
miR-506
GUGCCUU
miR-30
miR-384
UGUUUAC
5'-UGA
3'
71-77
88-94
327-333
untreat.
miR-NC
miR-124
miR-130
miR-384
miR-506
AR
β-actin
1.0
1.1
0.3
0.8
0.8
0.6
B
untreat
mock
miR-NC
miR-124
AR
PSA
β-actin
LNCaP
AR
PSA
β-actin
C4-2B
C
[miR-125b]
1.5
1.0
0.5
0.0
miR-NC
miR-124
C4-2B
cds2
D
RLU
120
100
80
60
40
20
0
60%
ΔBS3'UTR + + - -
3' UTR - - + +
miR-NC - - + -
miR-124 - + - +

Fig. 1

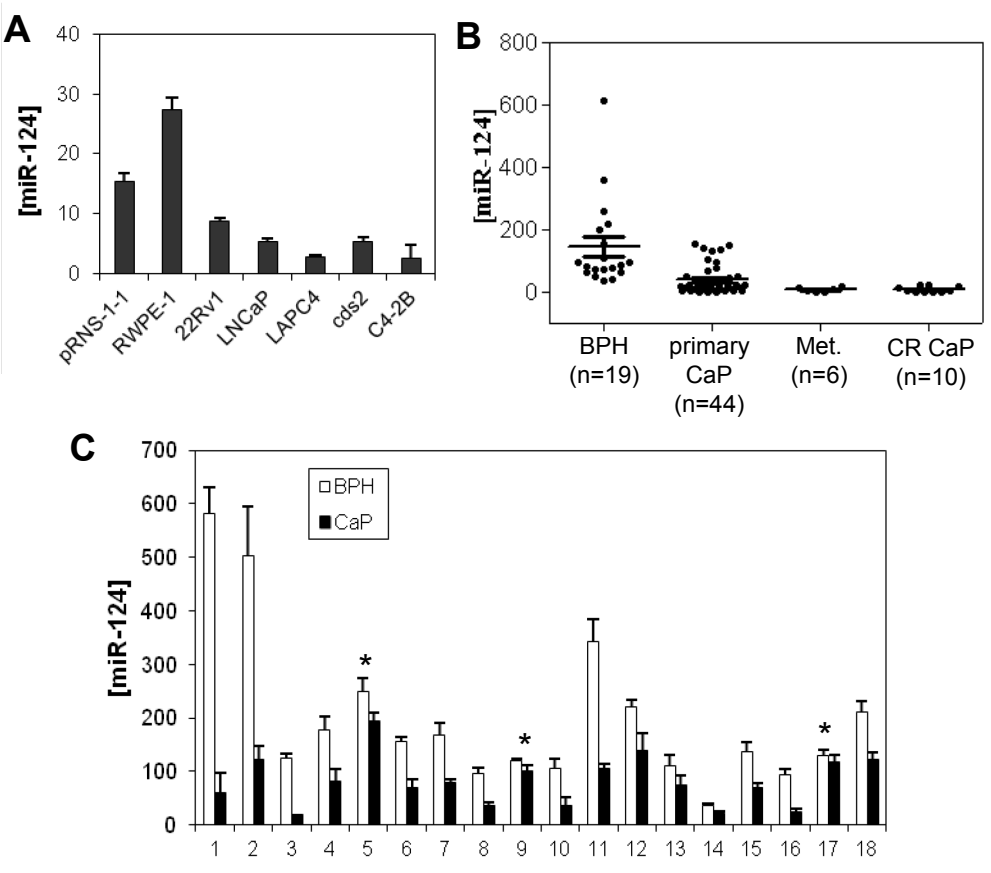
A
[miR-124]
40
30
20
10
0
pRNS-1-1
RWPE-1
22Rv1
LNCaP
LAPC4
cds2
C4-2B
B
[miR-124]
800
600
400
200
0
BPH (n=19)
primary CaP (n=44)
Met. (n=6)
CR CaP (n=10)
C
[miR-124]
700
600
500
400
300
200
100
0
BPH
CaP
*
*
*
1
2
3
4
5
6
7
8
9
10
11
12
13
14
15
16
17
18

Fig. 2

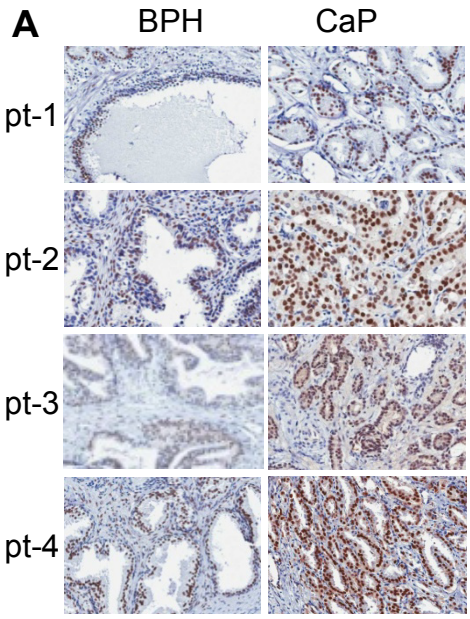
A
BPH
CaP
pt-1
pt-2
pt-3
pt-4

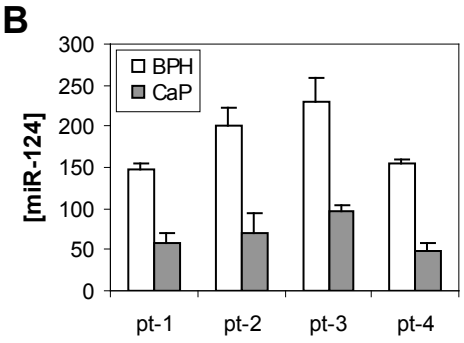
B
[miR-124]
300
250
200
150
100
50
0
BPH
CaP
pt-1
pt-2
pt-3
pt-4

Fig. 3

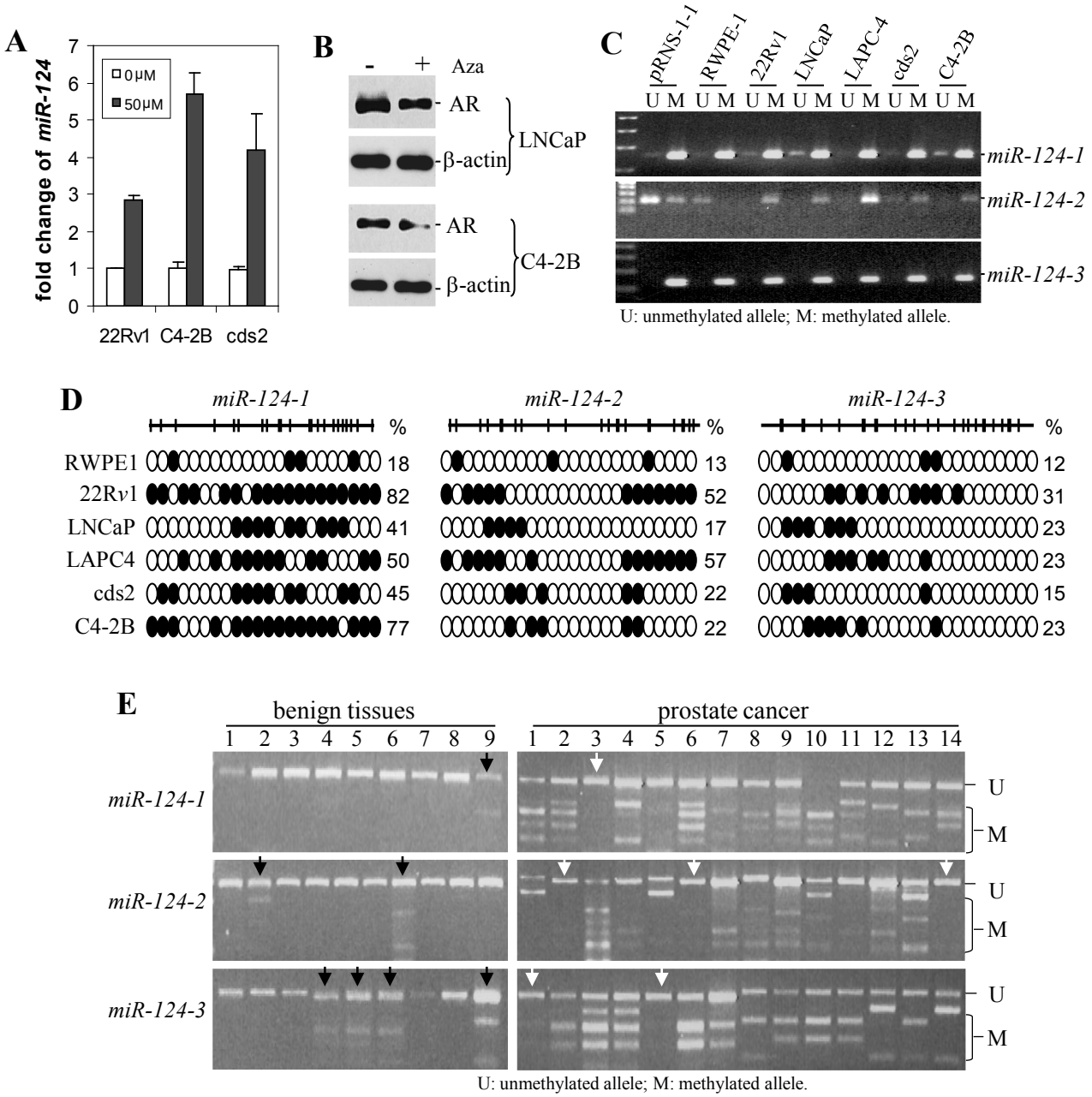
A
fold change of miR-124
0μM
50μM
22Rv1 C4-2B cds2
B
- + Aza
AR
β-actin
LNCaP
AR
β-actin
C4-2B
C
pRNS-1-1
RWPE-1
22Rv1
LNCaP
LAPC-4
cds2
C4-2B
U M U M U M U M U M U M U M U M
miR-124-1
miR-124-2
miR-124-3
U: unmethylated allele; M: methylated allele.
D
miR-124-1
miR-124-2
miR-124-3
%
RWPE1 18 13 12
22Rv1 82 52 31
LNCaP 41 17 23
LAPC4 50 57 23
cds2 45 22 15
C4-2B 77 22 23
E
benign tissues
prostate cancer
1 2 3 4 5 6 7 8 9
1 2 3 4 5 6 7 8 9 10 11 12 13 14
miR-124-1
miR-124-2
miR-124-3
U
M
U: unmethylated allele; M: methylated allele.

Fig. 4

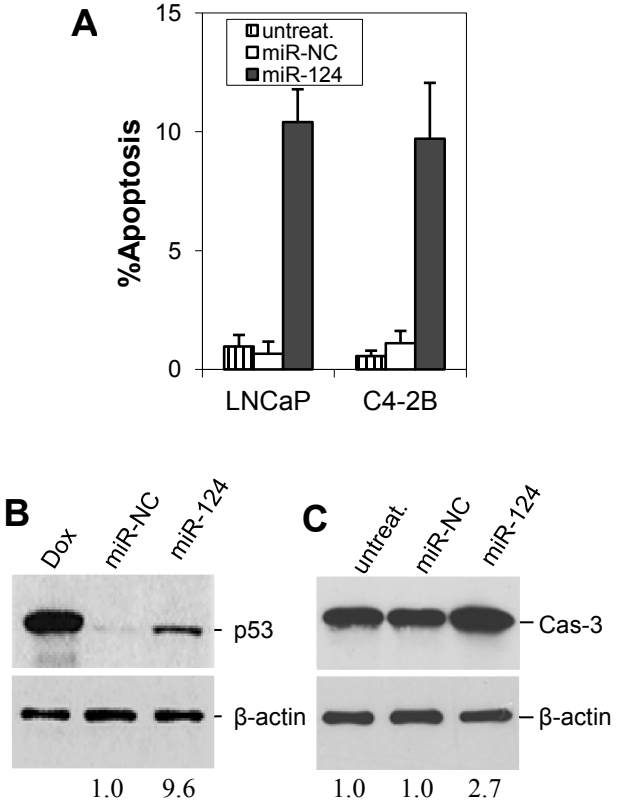
A
15
10
5
0
%Apoptosis
untreat.
miR-NC
miR-124
LNCaP
C4-2B
B
Dox
miR-NC
miR-124
p53
β-actin
1.0
9.6
C
untreat.
miR-NC
miR-124
Cas-3
β-actin
1.0
1.0
2.7

Fig. 5

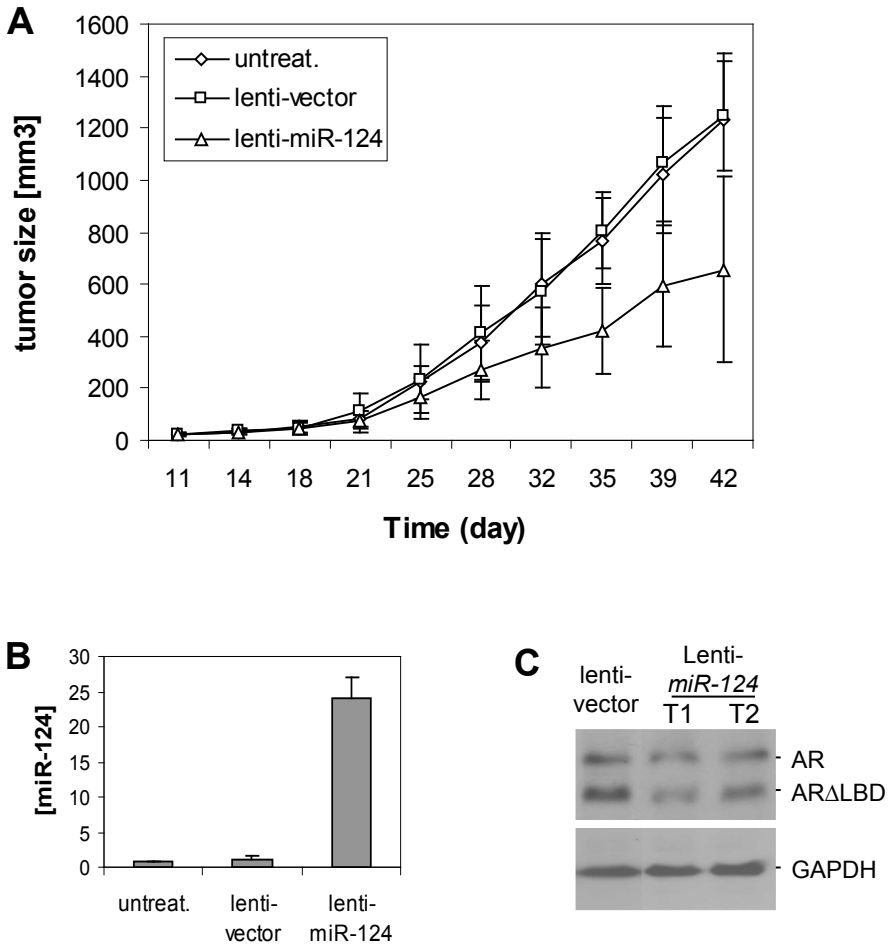
A
tumor size [mm3]
1600
1400
1200
1000
800
600
400
200
0
untreat.
lenti-vector
lenti-miR-124
11
14
18
21
25
28
32
35
39
42
Time (day)
B
[miR-124]
30
25
20
15
10
5
0
untreat.
lenti-vector
lenti-miR-124
C
lenti-vector
Lenti-miR-124
T1
T2
AR
ARΔLBD
GAPDH

Fig. 6

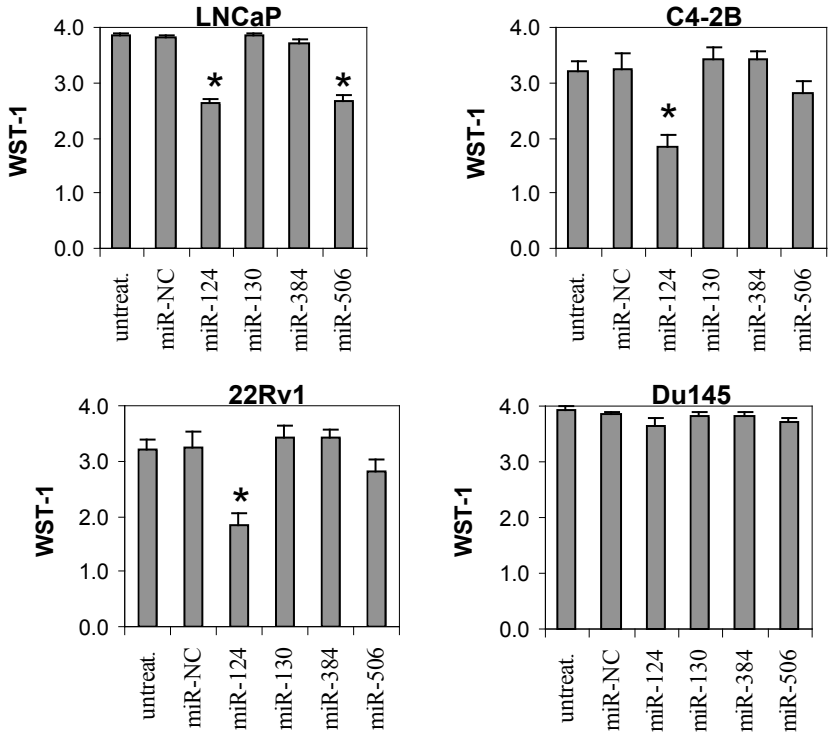

SI Figure 1. *miR-124* inhibits the proliferation of CaP cells. WST-1 cell proliferation analysis of AR-positive CaP cell lines. Cells (4 10^3 per well) were plated in 96-well plates for 24 hours, and then transfected with 100 nM synthetic miRNA mimics (miR-124m, miR-130m, miR-384m or miR-506m) or miRNA negative control (miR-NC) using lipofectamine 2000 (Invitrogen). The transfection protocol was optimized using a fluorescent pEGFP-N1 vector (Clontech) to ensure a transfection efficiency >90%. WST-1 cell proliferation assay was carried out at Day 5 after transfection. The growth changes were demonstrated as M SD (n = 3). AR-negative DU-145 cells were used as control that shows a slight inhibition of proliferation caused by miRNA mimics. "*" indicates a significant difference ($p<0.05$) relative to miR-NC.

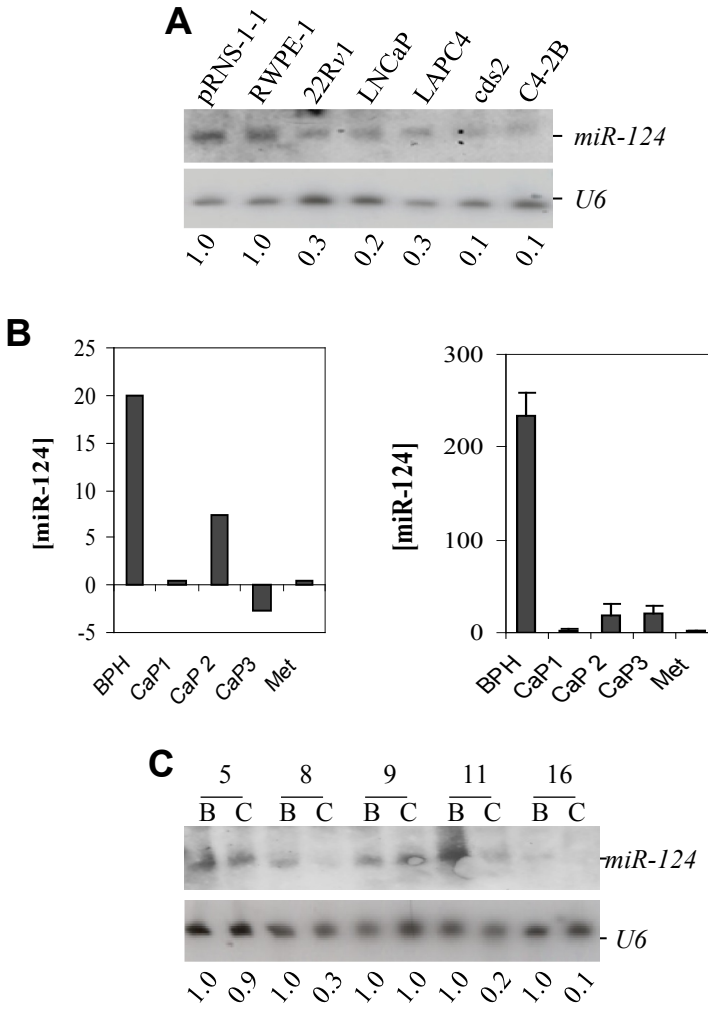

SI Figure 2. Downregulation of *miR-124* in CaP cell lines and in clinical specimens. *A*) To validate the qPCR results shown in Figure 2A, Northern blot assay was performed for *miR-124* expression in seven prostate cell lines (two benign and five malignant). The *miR-124* expression pattern is similar to that observed in qPCR. The numbers under the gel are the fold changes of *miR-124* in CaP cells (22R*v*1, LNCaP, LAPC4, cds2 and C4-2B) relative to in benign cells (pRNS-1-1 and RWPE-1). *B*) The expression levels of *miR-124* in one BPH and four CaP tissues (including a lymph node metastasis, Met) was summarized from a previous microarray profiling assay (*left*). The *miR-124* levels detected in the microarray profiling were validated by qPCR (*right*). *C*) Northern blot assay for *miR-124* in five CaP specimens that have sufficient amount of RNA. Three CaP samples (8, 11 and 16) having low *miR-124* levels detected by qPCR exhibit lower signal intensity in North blots, compared to their BPH matches. Two CaP samples (5 and 9) and their BPH matches exhibit similar signal intensity in North blots. The numbers under the gel are the fold changes of *miR-124* in CaP cells relative to in benign cells. B, BPH; C, CaP. *U6* was used as loading control.

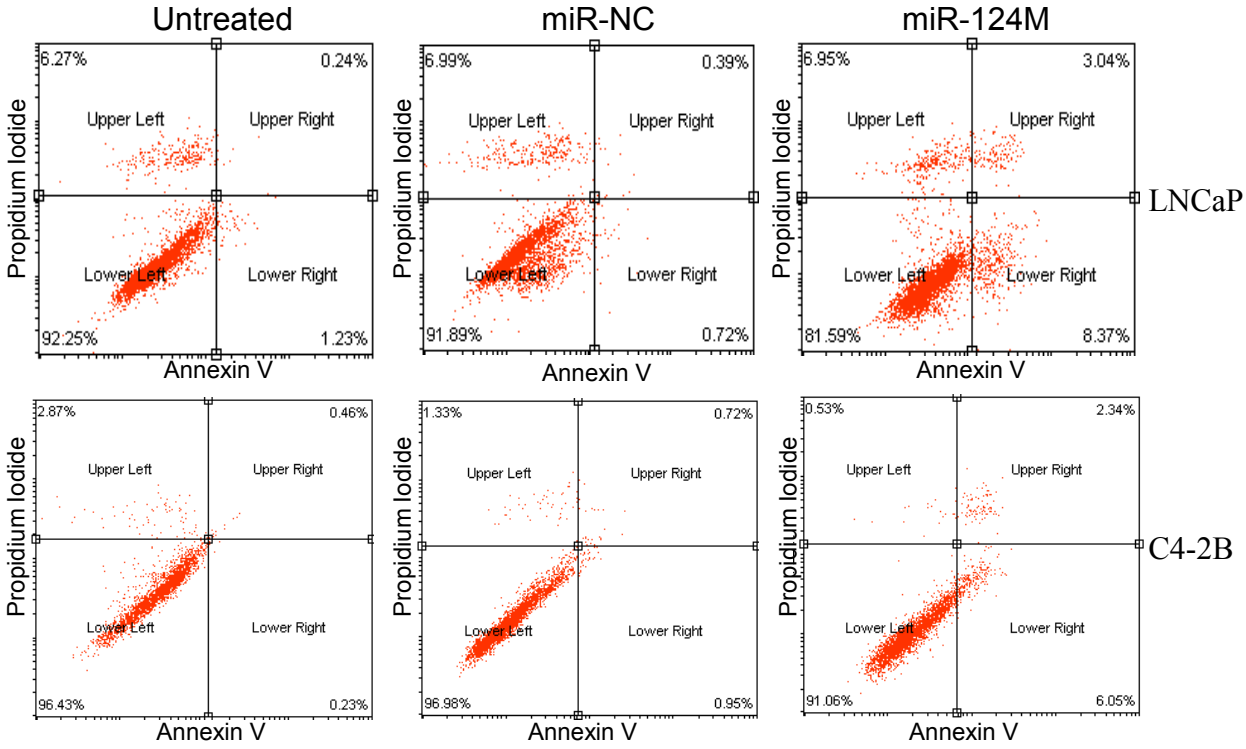

SI Figure 3. LNCaP (*top*) and C4-2B (*bottom*) cells transfected with 100 nM of miR-124m or miR-NC were grown in 10% FBS medium for four days. Both early apoptosis and later apoptosis were analyzed using Annexin V apoptosis assay protocol.

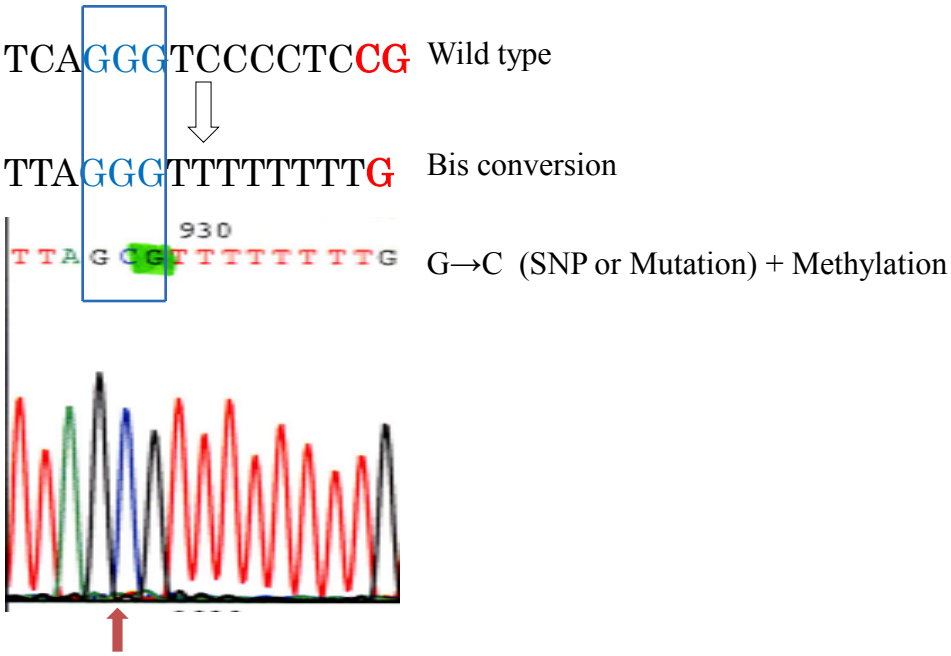

SI Figure 4. A point mutation or single nucleotide polymorphism (SNP) was detected at the 5'CpG region (1267 upstream of pre-miR-124-2) in a clinical CaP specimen. The wild-type "G" changed to "C" and was methylated (pointed out by an arrow).

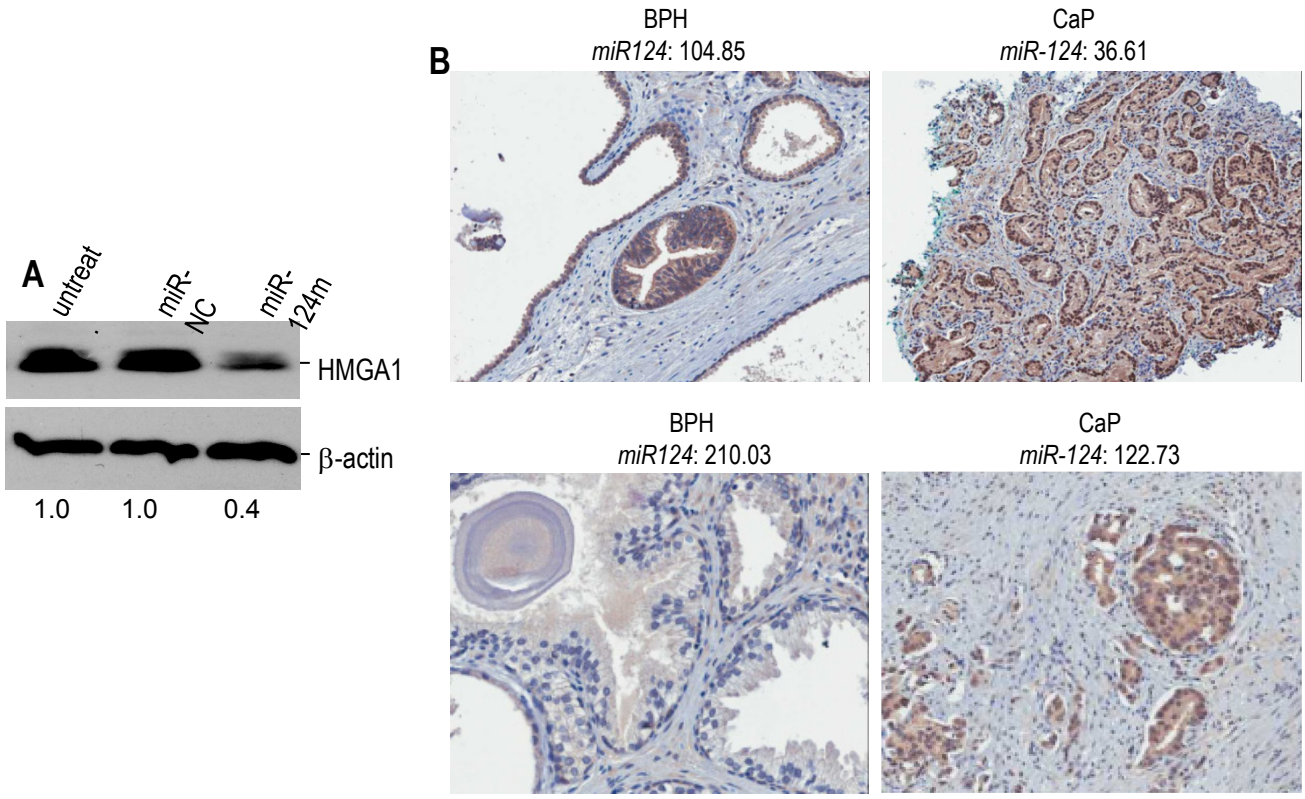

SI Figure 5. Analyses of the expression of HMGA1 in CaP cells. *A*) Western blotting analysis of HMGA1 expression in 100 nM miR-124m-transfectd C4-2B cells. The numbers under the gels are the fold changes of HMGA1 in miR-124m-treated C4-2B cells relative to miR-NC-treated cells. Our pilot results indicate that miR-124m treatment induced the downregulation of HMGA1 by ~60%. *B*) Immunohistochemical analysis of the expression of HMGA1 in two matched BPH and CaP tissues. CaP samples (*right*) and their BPHs (*left*) were immunostained using anti-HMGA1 antibody (sc-26348, Santa Cruz Biotechnology, Inc.). The abundance of *miR-124* in these tissues was measured using qPCR, and the values are shown on the top of each image. CaP tissues express lower level of *miR-124* than BPHs. Immunostaining for HMGA1 is more intense in two CaP samples than that in BPH matches. Moreover, localization of HMGA1 in the cytoplasm of CaP cells was obvious compared to that in BPH calls.